Research
Green Chemical Engineering: Soft Matter—Review

Ionic Elastomers for Electric Actuators and Sensors

Chenrun Feng [a,b,#], C.P. Hemantha Rajapaksha [c,#], Antal Jákli [a,b,c,*]

[a] Materials Science Graduate Program, Kent State University, Kent, OH 44242, USA
[b] Advanced Materials and Liquid Crystal Institute, Kent State University, Kent, OH 44242, USA
[c] Department of Physics, Kent State University, Kent, OH 44242, USA

ABSTRACT

In the past decades, ion conductive polymers and elastomers have drawn worldwide attention for their advanced functions in batteries, electroactive soft robotics, and sensors. Stretchable ionic elastomers with dispersed soft ionic moieties such as ionic liquids have gained remarkable attention as soft sensors, in applications such as the wearable devices that are often called electric skins. A considerable amount of research has been done on ionic-elastomer-based strain, pressure, and shear sensors; however, to the best of our knowledge, this research has not yet been reviewed. In this review, we summarize the materials and performance properties of engineered ionic elastomer actuators and sensors. First, we review three classes of ionic elastomer actuators—namely, ionic polymer metal composites, ionic conducting polymers, and ionic polymer/carbon nanocomposites—and provide perspectives for future actuators, such as adaptive four-dimensional (4D) printed systems and ionic liquid crystal elastomers (iLCEs). Next, we review the state of the art of ionic elastomeric strain and pressure sensors. We also discuss future wearable strain sensors for biomechanical applications and sports performance tracking. Finally, we present the preliminary results of iLCE sensors based on flexoelectric signals and their amplification by integrating them with organic electrochemical transistors.

1. Introduction

Actuators and sensors convert one form of energy into another suitable form of energy, which can be mechanical, thermal, electrical, optical, or magnetic [1–10]. Materials that respond (i.e., by changing shape or size) to an external stimulus, such as electric [11–19] and magnetic fields [20], heat [21–23], pressure [24,25], pH [26,27], and light [17,28–32], can be used for sensors and actuators. For device applications, which can be easily manipulated and adapted for computational controls, all those energy forms are preferably converted into electric signals. In this review, we will concentrate on electromechanical actuators that convert electric signals into mechanical responses (i.e., strains, pressure) and sensors that convert mechanical signals (i.e., strains, pressure) into measurable electric signals (i.e., current, voltage, resistance, or capacitance). Specifically, we will concentrate on rubber-like polymers (so-called elastomers) that have a low Young's modulus and

high failure strain, such that they combine softness with elasticity; that is, they are reversibly deformable. We will also focus on the latest results of liquid crystal elastomers (LCEs), which combine the orientational order of liquid crystal (LC) mesogens with the soft elasticity of polymer networks. LCEs can deform in response to diverse external stimuli, such as light [33], heat [34], and electric fields [35].

Electrically insulated electromechanical transducers based on dielectric elastomers [36,37], ferroelectric polymers [38], and LCEs [39,40] are promising for soft robotics due to their light weight, easy and inexpensive manufacturing, and high corrosion resistance [41–43], although they require high electric fields (several kilovolts per millimeter) [12] for sizable actuation [11,44].

The combination of elastomeric and ionic entities with unique and compelling properties provides impressive candidates for flexible/wearable sensors and actuators for human motion monitoring [45–48], soft robotics [49–52], health monitoring [51], prosthetics [51], and smart clothes [47]. Polymeric ion conductors have been developed for years as conducting electrodes and electrolytes [50], where devices combine both mobile ions and electrons. The rapid demand for highly conductive ionic elastomers in recent iontronics has provided a large selection of materials such as photo/

thermo-crosslinked ion conductive elastomers and differently sized organic/inorganic ions [53–56].

Ionic electroactive polymers (iEAPs) and elastomers (iEAEs) that use ion transport to facilitate electromechanical coupling with low voltage operation and large response signals have drawn widespread attention for their advanced functions in batteries, electroactive soft robotics, and sensors [57]. The movement of negative and positive ions with different sizes in opposite directions, either in an applied local electric field or due to bending deformations, can generate electric capacity for energy harvesting or convert electric energy into mechanical deformations. This electromechanical coupling mechanism has been found in natural elastomeric systems such as neuromuscular activities in electric eels and squids, which convert shape deformation into electric signals for sensing and, inversely, use electric signal to actuate muscles. The knowledge we have learned from natural systems is beginning to be utilized in soft robotics [58–60], skin sensors [61], and artificial intelligence technologies [62].

Salts with a melting point below room temperature (called ionic liquids (ILs)), which typically consist of a bulky organic cation and a smaller inorganic/organic anion, are suitable ionic components of iEAEs. Their high conductivity, low toxicity, wide electrochemical windows, optical transparency, low volatility, high thermal stability, and good electrochemical stability [63–65] make ILs suitable for many applications in electrochemical sensors [64,66,67], energy devices [68–71], and actuators [55,72,73]. In addition, they are nonirritant to skin and eye, non-sensitizing, and non-mutagenic. These properties can be tuned to a certain extent by changing the combination of cations and anions [74,75]. The host elastomers are compatible with three-dimensional (3D) printing technologies [76–78], and are capable of being used to create micro-/nano-structures [79,80], self-healing [81–84], and even self-powering [84], thereby offering more flexibility for advanced robotic and sensor technologies.

A considerable amount of research has been performed on ionic-elastomer-based strain [47,48,51,52,85], pressure [48,86–89], and shear [90] sensors. However, the reviews of research on ionic elastomers are sparse [91–94], thus justifying this review, in which we summarize the materials and performance properties of engineered ionic elastomer actuators and sensors. In Section 2, we review three classes of ionic elastomer actuators: ionic polymer metal composites (IPMCs), ionic conducting polymers (ICPs), and ionic polymer/carbon nanocomposites (IPCNs). At the end of that section, we provide perspectives for future actuators, such as adaptive four-dimensional (4D) printed systems and ionic liquid crystal elastomers (iLCEs). Section 3 is devoted to ionic elastomeric strain and pressure sensors. We also discuss future wearable strain sensors for biomechanical applications and sports performance tracking. At the end of Section 3, we present the preliminary results of iLCE sensors based on flexoelectric signals and their amplification by integrating them with organic electrochemical transistors (OECTs). Finally, we provide a short summary with an illustration of the interplay between action, perception, and adaption that will be integral parts of future ionic elastomer actuators and sensors.

2. Ionic elastomer actuators

Typical ionic elastomer actuator systems are composed of an elastomeric electrolyte with different sizes of cations and anions, sandwiched between two counter electrodes [15]. In this system, even weak, low-frequency, or direct current (DC) electric fields cause the drift of ions in opposite directions, leading to an expansion (compression) at one side, where the larger (smaller) ions move to, and causing considerable bending in thin ionic elastomer films. Due to the bidirectional and low voltage actuation, ionic

elastomer actuators are being considered for soft robotics, space exploration, and naval and biomedical applications.

The size-independent strain (ε) generated by the applied voltages can be calculated by $\varepsilon = (2dw)/\left(L^2 + d^2\right)$ [95,96], where d is the tip displacement in the horizontal direction, L is the length, and w is the thickness of the film. The parameters that characterize the performance of ionic elastomer actuators are the strain, stress, frequency range (bandwidth), and safe operating window of the electric actuation. These parameters mainly depend on the ionic conductivity, ion-exchange capacity, and electrochemical and mechanical stability of the ionic elastomer electrolytes, as well as on the electric conductivity, electrochemical stability, mechanical compliancy, and durability of the electrode materials. For device applications, the engineering design of the electrodes and electrolyte materials and their compatibility are the limiting factors.

2.1. Material design of ionic elastomer actuators

The chemical structures of the base polymers that are crosslinked to ionic elastomers are shown in Fig. 1.

The low-voltage actuation of ionic elastomers was first studied by Tanaka et al. [97] using poly(acrylic acid) gels as the base polymer, swollen in aqueous solvent environments. Due to their high ionic conductivity (10^{-1} S·cm^{-1}), aqueous ionic elastomer electrolytes, such as Nafion (Fig. 1(a)) or polyethylene oxide (PEO; Fig. 1(b)), coupled with alkali metal ions have large bending amplitudes and a fast response (a bandwidth of ~100 Hz), which make them suitable for underwater robotic applications [98–100]. Studies have found that the ion-water nano-clusters or channels formed inside elastomeric networks can facilitate ion transportation. However, the back relaxation and short cycle life limit the actuation performance.

Block-copolymers, such as poly((t-butyl-styrene)-b-(ethylene-r-propylene)-b-(styrene-r-styrene sulfonate)-b-(ethylene-r-propylene)-b-(t-butyl-styrene)) (tBS-EP-SS-EP-tBS; SSPB) pentablock copolymer (Fig. 1(c)) [101], poly(acrylic acid) (PAA)-co-poly(acrylonitrile) (PAN) (Fig. 1(d)) [102], and polyvinylidene fluoride (PVDF)-co-hexafluoropropylene (HFP) (Fig. 1(e)) [103], which have controllable phase-separated nanostructures, are used as ion-exchange membranes to enhance the mobility of the ions inside the elastomers and reduce back relaxations. For air-operated actuators, ILs with stable electrochemical properties and low volatility are usually desired. Examples of suitable ILs include 1-ethyl-3-methylimidazolium (EMI) tetrafluoroborate (BF$_4$) (EMI-BF$_4$), EMI bis(trifluoromethylsulfonyl)imide (TFSI) (EMI-TFSI), 1-butyl-3-methylimidazolium (BMI)-BF$_4$, 1-hexyl-3-methylimidazolium (HMI)-BF$_4$, 1-octyl-3-methylimidazolium (OMI)-BF$_4$, and HMI hexafluorophosphate (PF$_6$) (HMI-PF$_6$) (Fig. 1(f)) [104–106]. Due to the large molecular radii of organic ions, their ion mobility is poor when dispersed in elastomers.

To improve the actuation amplitude and blocking force, the abovementioned block-copolymers have been integrated with zwitterionic 3-(1-methyl-3-imidazolium) propanesulfonate (ZImS) (Fig. 1(g)) [16], single-walled carbon nanotubes (SWCNTs) [107,108] (Fig. 1(h)), halloysite nanoclays (HNCs) [102], silica nano-powders [109], or layered sulfonated montmorillonite (s-MMT) [110], in order to improve the ion transportation and mechanical strength of the elastomer membranes. In addition, poly(ionic liquid)/ionomers, such as ethylene oxide (EO) or hydrocarbon (HC) crosslinker-tethered imidazolium cations or TFSI anions [111,112], and imidazole-doped polystyrene sulfonate (PSS)-b-polymethylbutylene (PMB) (Fig. 1(i)) with vertically self-assembled hexagonal ionic channels across the film [16], have been synthesized to improve the ionic conductivity of IL-based elastomers [113].
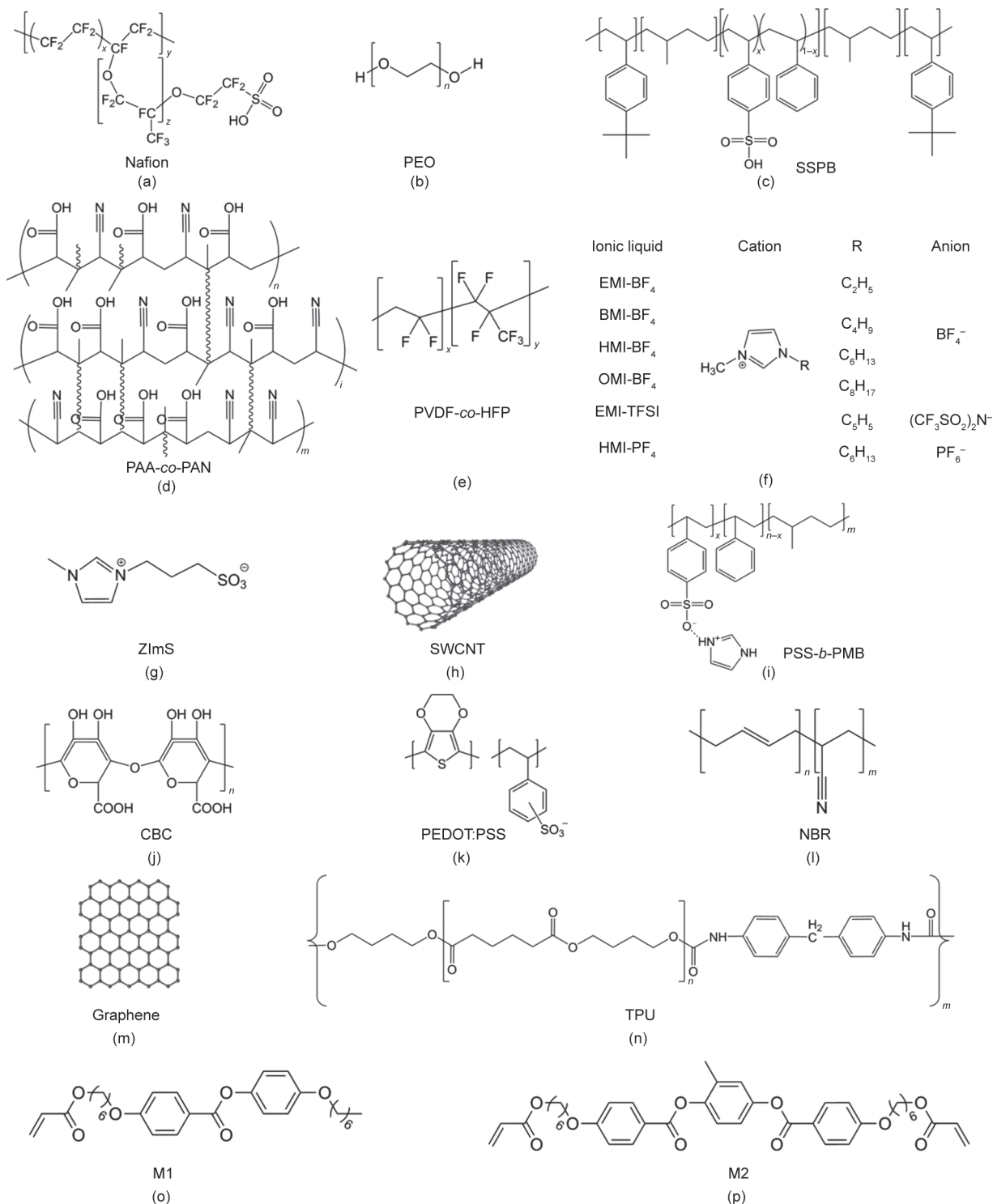
Fig. 1. Chemical structures of typical ionic elastomer materials used for ionic electroactive elastomers. (a) Nafion and (b) polyethylene oxide (PEO) are the most widely used base polymers of ionic elastomers, and (c) poly((t-butyl-styrene)-b-(ethylene-r-propylene)-b-(styrene-r-styrene sulfonate)-b-(ethylene-r-propylene)-b-(t-butyl-styrene)) (tBS-EP-SS-EP-tBS; SSPB), (d) poly(acrylic acid)-co-poly(acrylonitrile) (PAA-co-PAN), and (e) polyvinylidene fluoride-co-hexafluoropropylene (PVDF-co-HFP) are block-copolymers used in ionic elastomers. Part (f) summarizes most of the ILs used in ionic elastomers (EMI: 1-ethyl-3-methylimidazolium; BF$_4$: tetrafluoroborate; BMI: 1-butyl-3-methylimidazolium; HMI: 1-hexyl-3-methylimidazolium; OMI: 1-octyl-3-methylimidazolium; TFSI: bis(trifluoromethyl-sulfnyl)imide; PF$_6$: hexafluorophosphate). (g) Zwitterionic 3-(1-methyl-3-imidazolium) propanesulfonate (ZImS) and (h) single-walled carbon nanotube (SWCNT) are additives to improve the performance of ionic elastomers; (i) polystyrene sulfonate-b-polymethylbutylene (PSS-b-PMB) is a block-copolymer self-assembled with the ionic group in ionic elastomers; (j) carboxylated bacterial cellulose (CBC) is one of the biomaterials used in ionic elastomers; (k) poly(3,4-ethylenedioxythiophene) polystyrene sulfonate (PEDOT:PSS) and (l) nitrile butadiene rubber (NBR) are electrodes and base polymer interpenetrated networks; (h) SWCNT, (k) PEDOT:PSS, and (m) graphene are examples of electrode materials used in ionic elastomers; (n) thermoplastic polyurethane (TPU) is common rubbery material used in ionic elastomers; and (o) 4-(6-acryloxy-hex-1-yl-oxy)phenyl-4-(hexyloxy)benzoate (M1) and (p) 1,4-bis-[4-(6-acryloyloxyhexyloxy)benzoyloxy]-2-methylbenzene (M2) are liquid crystalline monomers used in ionic elastomers.

For biomedical/biodegradable applications, cellulose- [114] and chitosan-based [115] biomaterials, such as carboxylated bacterial cellulose (CBC) nano-fiber networks (Fig. 1(j)), have been utilized and exhibited good ionic conductivity and biocompatibility. To increase the compatibility between soft elastomers and electrodes, the electrodes were integrated with ionic elastomers, such as by polymerizing 3,4-ethylenedioxythiophene (EDOT) (Fig. 1(k)) with polyethylene oxide (PEO)/nitrile butadiene rubber (NBR) interpenetrating polymer networks (IPNs) (PEO/NBR-IPNs) [116,117], shown in Figs. 1(b) and (l).

A large variety of electrodes can be used to apply electric fields onto ionic elastomers, including metals, conducting polymers (CPs) (e.g., poly(3,4-ethylenedioxythiophene) (PEDOT):PSS; see Fig. 1(k)), and nano carbons (e.g., SWCNT and graphene; see Figs. 1(h) and (m)). The requirements for the speed and amplitude of the actuation will differ depending on the purpose of the actuator device; therefore, a number of advanced electrode and ionic elastomer membrane materials have recently been engineered and assembled together for various ionic elastomer electric actuator applications. Current ionic elastomer actuators can be classified into three major categories: IPMCs, ICPs, and IPCNs.

2.2. Ionic polymer metal composite actuators

IPMCs using ionic elastomer membranes sandwiched between two metallic electrodes have been one of the most widely used types of ionic elastomer actuators since the 1990s [118]. When applying a small electric field (a few volts per millimeter) across an elastomer, the differently sized ions or ion clusters stored inside the membrane will move from one side to the other, causing the actuator to bend (as one side will have a larger volume expansion than the other) [119,120]. Initially, due to their good ionic conductivity ($\sim$0.1 S·cm^{-1}), aqueous ionic elastomeric membranes such as Nafion [121] and Flemion [122], which contain anionic sulfonate and carboxylate groups [123,124], were used to provide a quick response for IPMCs [125]. These ionic elastomers operate in an electrolyte solution or in a swollen state, where fixed anionic groups create nano-channels as a gateway for alkali metal/ammonium cations (H^+, Li^+, Na^+, K^+, BMI^+) with water clusters to move inside [98,99], as shown in Fig. 2(a). Experiments on a Pt-Nafion actuator with different cations–water clusters showed that the smallest cations have the best ion migration with the highest water absorption, bending rate, and blocking force (Fig. 2(b)) [100]. However, the leakage and evaporation of water from the actuator as well as the poor electrochemical stability of aqueous electrolytes with a metallic electrode resulted in limited work density/force, back relaxation, and corrosion in air operation [105,126,127].

One strategy to fabricate IPMC actuators with stable air performance involves the use of hydrophobic ILs such as EMI-BF$_4$, EMI-TFSI, BMI-BF$_4$, HMI-BF$_4$, OMI-BF$_4$, and so forth (Fig. 1(f)) [104–106,128]. However, hydrophobic IL-based IPMCs suffer from a slow actuating response due to insufficient ionic conductivity under dry conditions. To enhance ion migration and the force generated by IPMCs, self-assembled block-copolymer–IL composite membranes, such as sulfonated poly(styrene-*b*-ethylene-*co*-butylene-*b*-styrene) (SSEBS) [129], PAA-*co*-PAN [102], and PVDF-*co*-HFP [103], were fabricated to form nano-structured ion channels inside the elastomeric networks via controllable phase separations [120]. In addition, various cationic and anionic radiation-grafted ion-exchange membranes, such as imidazolium-tethered triblock copolymers [130] with single-ion actuation, have been introduced in order to enhance the actuation amplitude and response time, and eliminate back relaxation [131].

Fig. 2(c) [101] illustrates the phase-separated ionic and non-ionic regions inside a novel penta-block-copolymer (SSBP) elastomer (Fig. 1(c)) with layered sulfonated montmorillonite (s-MMT) [110] nanocomposites. The microphase-separated morphology, with controlled ionic channels tens of nanometers wide inside the elastomer, increased the IL uptake amount and the ionic conductivity to more than double that of a Nafion/IL system. The additional interaction between s-MMT and the solvated ions created wider ion channels for mass transport and enhanced the elastic modulus to 89 MPa. When operating in air, this actuator exhibited a large bending strain of about 1.2% under 2 V of DC voltage without any back relaxations for 10 min.

The degree of actuation not only depends on the type of polymer and counter ions used, but also on the quality, thickness, and active surface area of the metal electrodes deposited on the ionic elastomer membranes. The first generation of IPMCs used chemically deposited platinum electrodes on the two sides of the electrolyte membrane [120,132,133]. Later on, other types of inexpensive and flexible metal electrodes, such as copper, palladium, silver, and gold, were prepared by means of physical and chemical deposition methods [134,135]. Metal electrodes have a low surface resistance and high current density, resulting in faster actuation ($\sim$0.1 s) and a larger bending strain (>3%) [136]. However, the poor compatibility of the interface between the electrode and the ionic elastomer membrane may result in electrode delamination, fatigue, and cracking, contrary to the stable performance of IPMC actuators [55,124,137]. The interfacial area can be optimized to enhance the charge accumulation and adhesion of metal electrodes by means of metallic nanoparticles with various sizes, shapes, and surface roughness [138–140]; in addition, metallic nanoparticles can be implanted into an intermediate layer [102,135,137,141]. Yan et al. [102] introduced supersonic cluster beam implantation (SCBI) [142] to implant roughly 100 nm thick cluster-assembled electrodes tens of nanometers beneath the surface of an ionic elastomer membrane with high electrical conductivity and stretchability (Figs. 3(a)–(c)). In this case, the ionic elastomeric electrolytes were made by PAA-*co*-PAN (Fig. 1(d)) networks blended with HNCs [143], along with tetraethyl ammonium cation (TEA$^+$) and ethylene glycol dimethacrylate crosslinkers. With additional IL EMI-BF$_4$ added as the transport medium for TEA$^+$ in the actuator system, the maximum actuation strain was increased to 1.04% at 5 V (Fig. 3(d)). Due to good adhesion and a sufficient interaction area for the gold nanocluster electrodes, the actuator responded up to 10 Hz and carried out 76 000 cycles at 2 V and 1 Hz without back relaxations or electrode cracks.

IPMCs with appropriate programming and engineering design are promising candidates for flapping actuators for flying/crawling robots [144–147], biomimetic robotic fish [148,149], and artificial joints with a multiple degrees-of-freedom manipulator [150]. Table 1 [98,100–102,108,122] summarizes the most important properties of IPMC actuators.

2.3. Ionic conducting polymer actuators

Conjugated polymers such as polypyrroles (PPy) [151], polyanilines (PANI) [152], polythiophenes (PT) [153], and PEDOT:PSS [154,155] can be used both as electrodes and as bulk elastomer actuators with volume changes. These conjugated polymers are conducting if doped with ions, and semiconducting if undoped [156,157].

A CP can be negatively charged (n-doped) with electrons inserted or positively charged (p-doped) with electrons extracted. When applying a small electric potential (0–30 V), cations or anions from the electrolyte move into p-doped (or n-doped) CP chains, causing a bulk volume expansion. If the direction of the electric field is reversed, the CP will contract as ions move out, as shown in Fig. 4(a) [41]. The linear and symmetric volume changes, with strains up to 40%, can be designed as actuators (Fig. 4(b) parts

(i) and (ii)), such as hollow tubes [116], textiles, and fibers [158]. However, operating bulk CP actuators often requires counter electrodes and surrounding electrolyte solutions. Tri-layer actuators comprised of an ionic elastomer membrane sandwiched between two CP layers are easier to fabricate, are able to operate under both dry and wet conditions, and perform bidirectional bending deformations with one electrode expanding and the other contracting

when a voltage is applied across the film (Fig. 4(b) parts (iii) and (iv)).

Among the various CPs, solution-processed PEDOT:PSS (Fig. 1(k)) has been commercialized. It is stable in air and easy to deposit via inkjet or 3D printing [159,160]. However, it has many limitations, such as slow response due to poor conductivity, and weak strain and stress due to small capacitance, resulting in weak
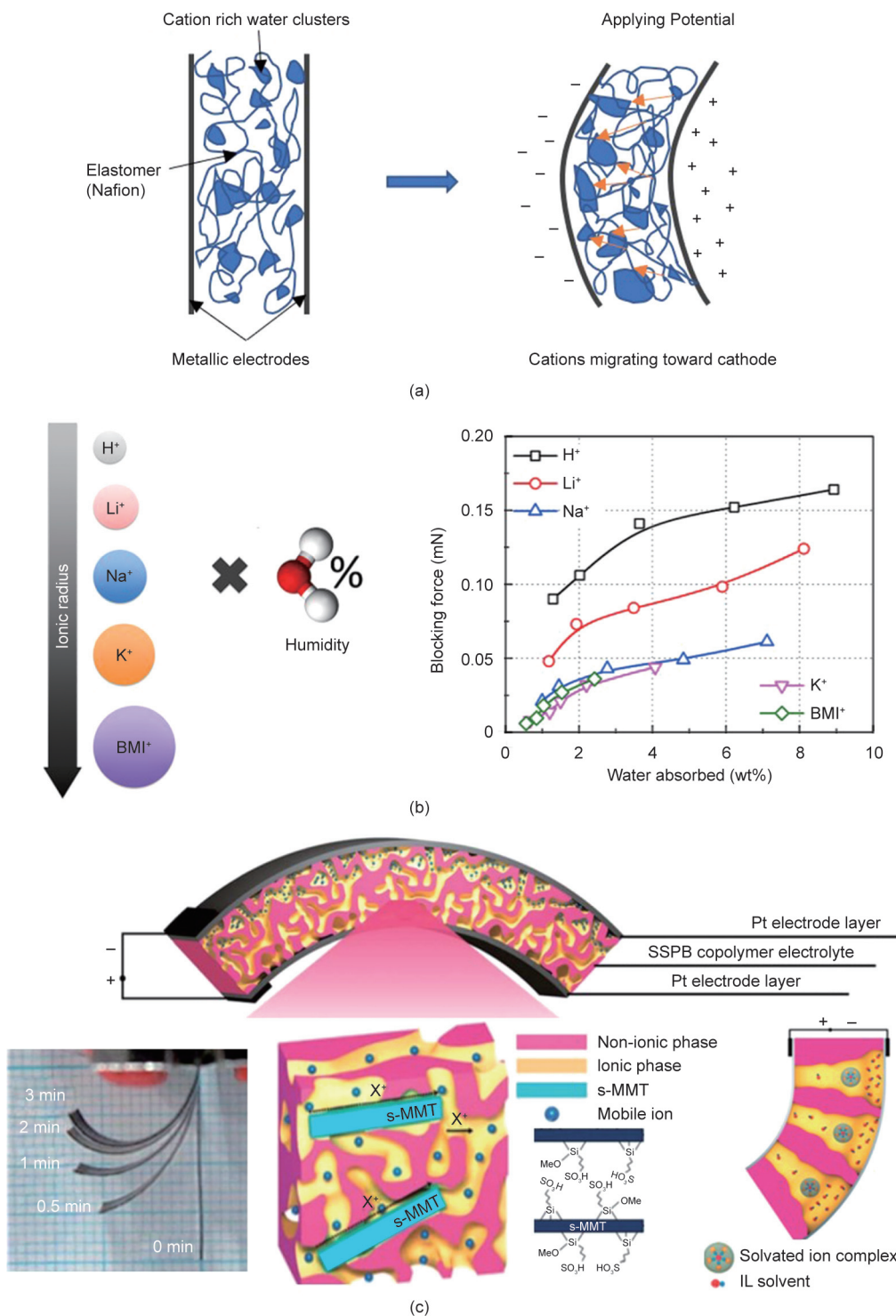

Fig. 2. Illustration of the performances of several IPMC actuators. (a) Sketch of the structure (left) and bending mechanism (right) of Pt-Nafion-based IPMC actuators. Blue-colored regions are nano-clusters formed by water–ion association inside Nafion-ionic elastomers. (b) Different sizes of cations inside Pt-Nafion actuators and their effect on performance. (c) Schematics of the engineering of phase-separated ionic elastomer actuators using a block-copolymer (SSPB) and s-MMT to enhance ion migration and volume expansion inside the elastomer membrane, as well as its bending performance under 5 V. (b) Reproduced from Ref. [100] with permission of Elsevier B.V., ©2020; (c) reproduced from Ref. [101] with permission of the Royal Society of Chemistry, ©2013.

electromechanical coupling efficiency. Studies show that the presence of ILs can enhance the conductivity and flexibility of CP electrodes [161]. Initially, in order to improve the ionic conductivity, a

metal layer was coated between the CP and ionic elastomer membrane [162]; however, delamination between the CP and metal limited the performance and lifetime. Instead of additional metal
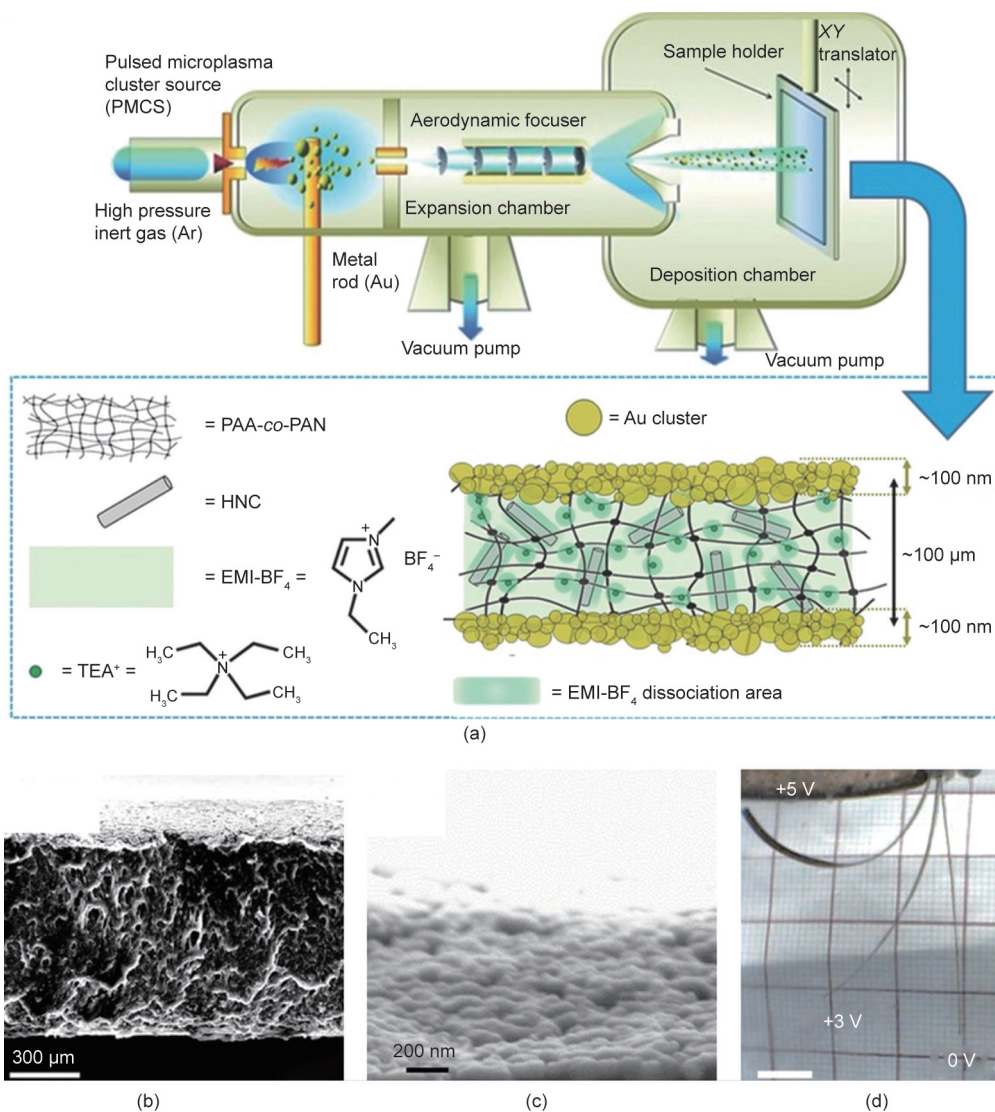

Fig. 3. PAA-*co*-PAN-based IPMC actuator with gold (Au) electrodes. (a) Illustration of the apparatus implanting gold nanocluster-assembled electrodes into the ionic elastomer membrane. (b) Scanning electron microscopy view of the cross-section of the actuator. (c) Nano morphology of the gold electrode surface. (d) Picture of the bending deformation of the actuator. Reproduced from Ref. [102] with permission of Wiley-VCH Verlag GmbH & Co. KGaA, ©2017.

Table 1
Summary of the most important parameters of selected IPMC actuators.

Elastome	Nafion/Flemion	PAA-*co*-PAN/HNC	SSPB/s-MMT	Nafion/MWCNT
Electrode	Pt	Au nano-clusters	Pt	Pt
Cation	H^+, K^+, Na^+, Li^+	TEA^+, EMI^+	HMI^+	H^+
Anion	Polymerized SO_3^-	BF_4^-	$TFSI^-$	Polymerized SO_3^-
Voltage (V)	< 5.0	5.0	2.0	4.5
Strain	> 1.50%	1.04%	1.20%	8°–12° bend
Blocking force (mN)	0.05 (K^+)–0.17 (H^+)	NR	NR	2.95–14.10
Response time (s)	0.01–0.1	0.1	NR	NR
Durability (cycles)	Low	76 000	NR	NR
Back relaxation	Yes	No	No	Yes
Elastic modulus (MPa)	70.00	0.35	4.10	NR
References	[98,100,122]	[102]	[101]	[108]

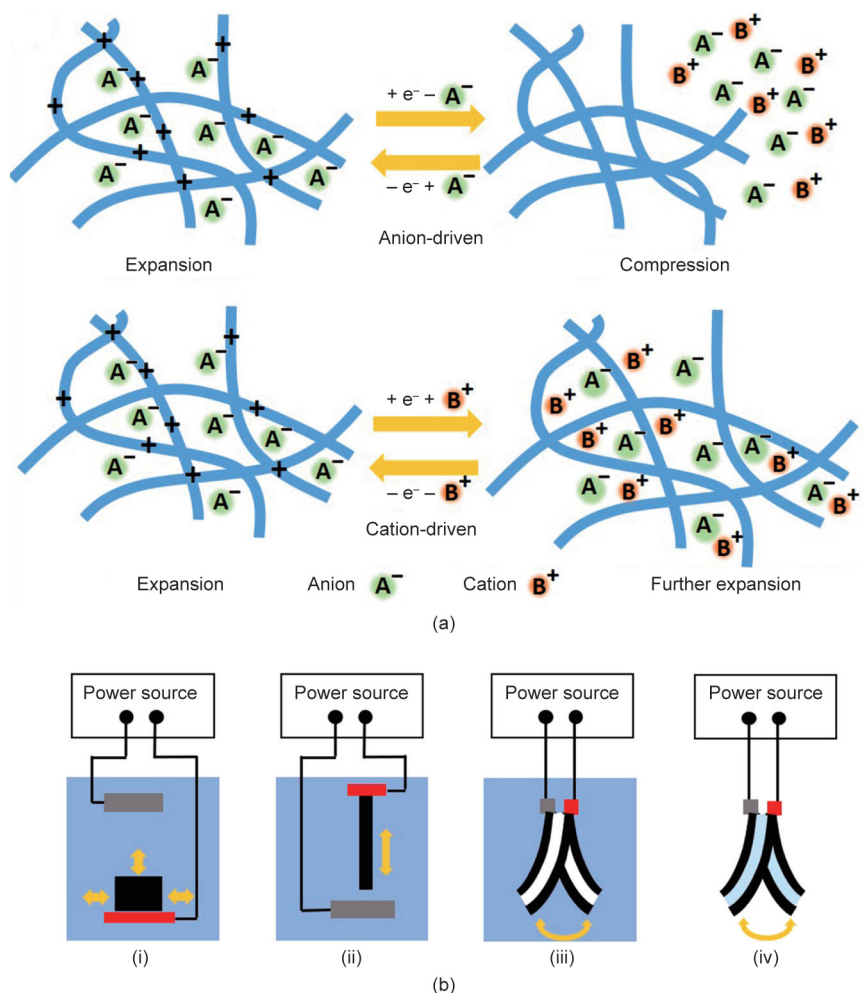MWCNT: multi-walled carbon nanotube. NR means "not reported."

Fig. 4. Schematics of ICP actuators. (a) Actuation mechanism of a p-doped CP. (b) Different types of deformation of CP actuators: (i) bulk expansion and compression; (ii) linear elongation and contraction; (iii) bending actuation under wet conditions; and (iv) bending actuation in air.

layers, nano materials such as silver (Ag) nanowires [163] or carbon nanotubes (CNTs) (Fig. 1(h)) are dispersed into the CP electrodes to enhance the conductivity and anisotropic mechanical strength. Wang et al. [155] reported a high-performance CP actuator based on multi-walled carbon nanotube (MWCNT)-dispersed PEDOT:PSS (M-PEDOT:PSS) electrode, as shown in Fig. 5(a).

The MWCNTs were inserted between the PEDOT and PSS polymer chains and aligned along the PSS chains by hydrogen bonding and π–π stacking. The resulting porous structure of the M-PEDOT:PSS electrodes improved the ion storage capacity (~100 F·g^{-1}), electrical conductivity (~150 S·cm^{-1}), and mechanical strength (~1 GPa), all of which were several times higher than those obtained with pure PEDOT:PSS electrodes. The performance of the ionic elastomer actuator using thermoplastic polyurethane (TPU), EMI-BF$_4$ IL, and M-PEDOT:PSS electrodes is compared with that of the same elastomer with PEDOT:PSS electrodes in Fig. 5(b) [164]. This actuator can perform 0.64% peak-to-peak actuation strain and 1.43 mN blocking force under 2.5 V and has a lifetime of up to 1 × 10^5 cycles under 1 Hz.

To reduce the delamination, additional interfacial polymeric layers were applied between the conjugated polymer electrodes and the ionic elastomer [165]. Good adhesion and compliant elasticity between the ionic elastomer membrane and the CP electrodes were achieved by integrating ion conductive PEO-based IPNs with PEDOT electrodes [166–168], as shown in Fig. 5(c). The phase-separated nanostructure of the PEO/NBR (Figs. 1(b) and (l))

IPN membrane provided high ionic conductivity (up to 10^{-3} S·cm^{-1}) and up to 2.4% peak-to-peak bending strain with PEDOT electrodes interpenetrated [167]. As the bending strain and mechanical strength of the actuator can be tuned by adding different amounts of polystyrene (PS) component, IPN actuators can be engineered into tubular-shaped surgical catheters for vessels and neurons [169], as well as linear and bending fibers for textile actuators [170,171]. The actuation capacity of these IPN actuators, which is up to 1 kHz [172], can be used as the wings of flying robots (Fig. 5(d)) [164].

CP actuators using biocompatible and biodegradable materials are suitable for origami applications and biomedical microrobots; for example, porous bacterial cellulose (BC) membranes with PEDOT:PSS electrodes [114,173] and cellulose paper with PPy or PANI electrodes [174] exhibited a quick response, no back relaxation, good mechanical strength, and large bending deformation.

Since the doping of conjugated polymers has a direct effect on colors, mechanical properties, conductivity, volume, and the porosity of the electrodes, CP actuators have wide variety of applications, such as in linear/bending fibers, diaphragms/micropumps, light-emitting diodes, swimming robots, drug delivery, active catheters, lens, batteries, supercapacitors, electrochromic devices, selective membranes, braille displays, microelectronics, sensors, and more [175,176]. Table 2 [114,155,162,167,172] summarizes the most important properties of ionic CP actuators.
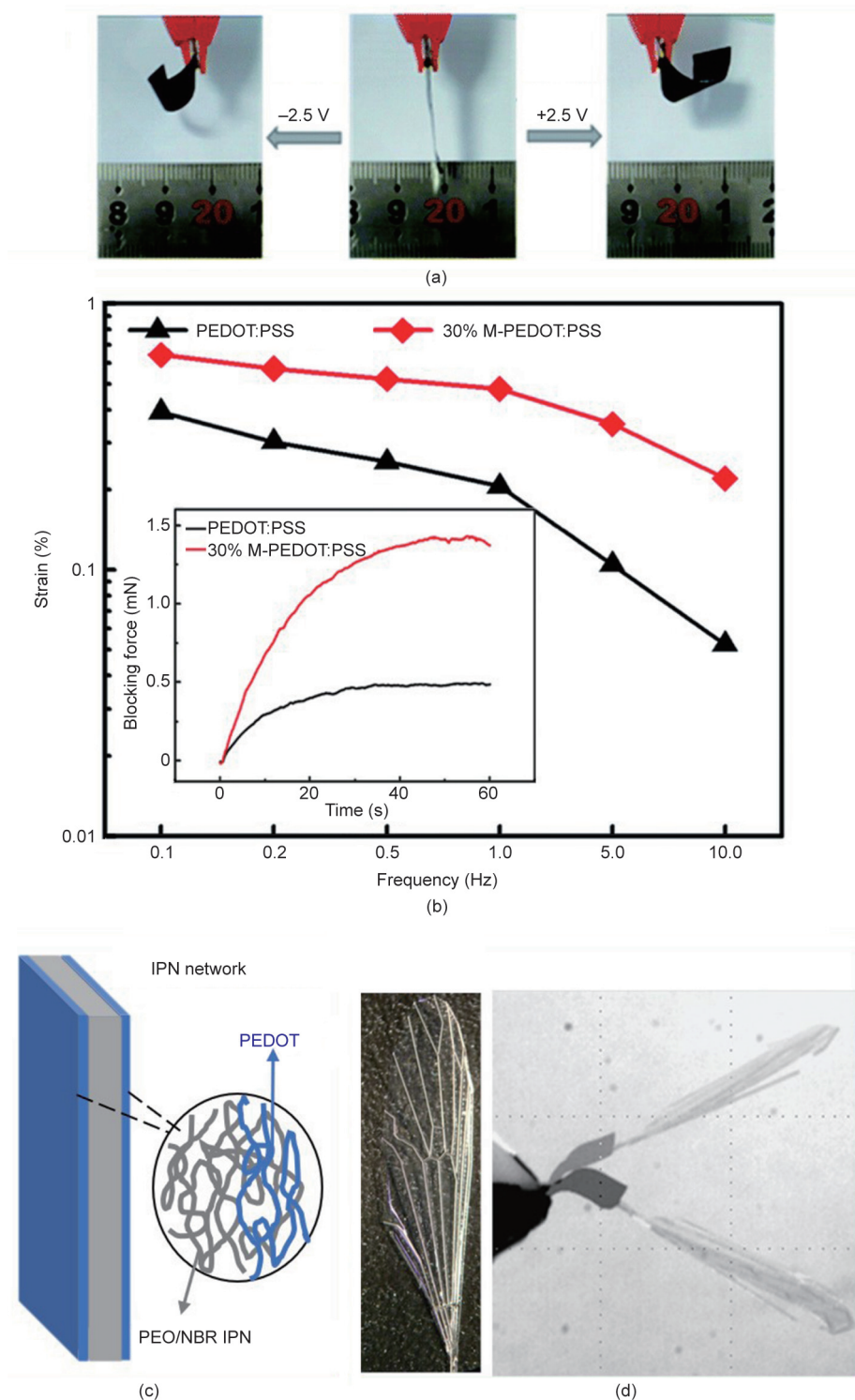
Fig. 5. Illustration of CP actuators. (a) Performance of bending actuation under ±2.5 V. (b) Bending strain at different frequencies of TPU:EMI-BF$_4$ ionic elastomer sandwiched by hot pressing between MWCNT-dispersed PEDOT:PSS (M-PEDOT:PSS) electrodes. Inset: time dependence of the blocking force. (c) Schematic nanostructure and (d) application as a bio-mimic vibrating wing of PEO-based tri-layer IPN actuators. (a, b) Reproduced from Ref. [155] with permission of the Royal Society of Chemistry, ©2017; (d) reproduced from Ref. [164] with permission of Wiley-VCH Verlag GmbH & Co. KGaA, ©2019.

2.4. Ionic polymer/carbon nanocomposite actuators

Nonmetallic nanomaterials such as CNTs [115,177], graphene [178–180], and graphitic carbon nitride [181] have been developed into electrode materials for IPCN bending actuators. These nanopowders are inexpensive (< 100 USD·kg^{-1} for graphene at present)

compared with gold or platinum, are easy to coat onto ionic elastomers by means of casting or self-assembly, and form very compliant electrodes with high specific surface area and stability [182].

The first IPCN actuators were bucky-gel actuators composed of SWCNT electrodes, an IL, and base elastomers [128,183–185]. The CNT electrodes are dispersed into ionic elastomers or directly

Table 2
Summary of the most important parameters of selected ICP actuators.

Elastomer	TPU	PEO/NBR-IPN	PVDF	CBC-NFN
Electrode	PEDOT:PSS/MWCNTs	PEDOT	PPy/Pt	PEDOT:PSS
Cation	EMI^+	EMI^+	TBA^+	EMI^+
Anion	BF_4^-	$TFSI^-$	PF_6^-	BF_4^-
Voltage (V)	2.5	2.0	2.0	2.5
Strain (%)	0.32	1.20	2.00	0.06
Blocking force (mN)	1.43	30	NR	NR
Response time (s)	0.1	0.001	1	2
Durability (cycles)	100 000	NR	3 600	360
Back relaxation	No	No	NR	No
Elastic modulus (MPa)	7.75	30.00	NR	44.26
References	[155]	[167,172]	[162]	[114]

NFN: nano-fiber network; TBA: tetrabutylammonium.

deposited onto the surface to assemble a tri-layer-type actuator [186–188]. Fast-switching bucky-gel actuators were demonstrated by Kim et al. [16] using hexagonal nano-structured PSS-*b*-PMB block-copolymers (Fig. 1(i)) with imidazolium cations bonded as single-ion actuation elastomers. With the additional zwitterion ZImS (Fig. 1(g)) to improve cation transportation, the actuator can bend with several times larger strain (1.8%, at ±3 V) and has a response about 100 times faster (20 ms) than that of the PVDF-*co*-HFP/Nafion-based bucky-gel actuators. In ionic elastomer actuators with carbon-based electrodes, the bending is attributed to the asymmetric charge injection to the CNT cathode and anode; therefore, the capacity and conductivity of the electrodes are the key factors in the bending strain/stress and response time. To increase the charge carriers and active surface areas, various nano-carbons with porous structures, such as carbide-derived carbon [189–191], activated carbon nanofiber [192], carbon aerogels [193], MWCNTs [194], and nanoporous carbon [195], have been used in the electrodes. In addition, the capacity of the electrode layers can be increased by adding nanoparticle additives, such as meso-porous silica (MCM), PANI, and carbon black into CNT-based bucky gels with large strain (1.9%, ±2 V) and strength (8.8 MPa) [196]. However, the electrical conductivity of nano-carbon materials is lower than that of metal electrodes, and metal backing is usually required to boost the electrical conductivity [175]. Vertically aligned (VA) SWCNT electrodes [177,197] can be directly deposited onto the ionic elastomer layer by means of chemical vapor deposition (CVD) [188]. The high electrical conductivity, fast ion conduction, and strong elastic modulus due to the continuous paths through VA-CNT channels in the actuator enhance the bending strain by over 8% and the actuation speed to 10% strain per second under a voltage of 4 V.

Later, a number of hierarchical nano-structured carbon electrodes were designed to improve the performance of the IPCN actuators [115,198]. Wu et al. [199] prepared hierarchical black-phosphorous (BP)-based CNTs as the electrodes of a PVDF-*co*-HFP (Fig. 1(e))-based tri-layer actuator. The electrode has an ordered lamellar structure with a large interacting area and capacitance for smooth ion transportation, as shown in Fig. 6(a) [199]. The enhanced capacity of the BP-CNT layering electrodes produced a peak-to-peak bending strain of about 2%, with a fast response of up to 20 Hz (Fig. 6(b)). Actuators with an appropriate engineering design can be used as vibrating wings or artificial grabbing hands. Two-dimensional (2D) materials, such as graphene nanosheets (Fig. 1(m)) with intercalated ions and well-aligned structures, exhibit an even larger surface area, transparency, and volume expansion (> 700%) than those of CNT electrodes, although the restacking of graphene layers reduces the lifetime [103]. Lu et al. [200] doped Ag nanoparticles into reduced graphene oxide (rGO) to enhance the conductivity and alignment stability of the electrodes, leading to a high-frequency bending actuator. Recently,

ionically crosslinked MXene (2D layers of transition metal carbides, nitrides, or carbonitrides) has been used as electrodes with high conductivity and capacity. Electrodes using $Ti_3C_2T_x$–PEDOT:PSS ($Ti_3C_2T_x$–PP) (Fig. 6(c)) [201] with ordered layered structures enhance the volumetric capacitance to about 1 $kF\cdot cm^{-3}$, yielding fast ionic conduction in Nafion-based ionic elastomer actuators. The resulting actuator exhibited a sub-second rise time and a strain of up to 1.37% peak-to-peak bending at 1 V up to 20 Hz, good flexibility, and stability at up to 18 000 cycles without delamination. Fig. 6(d) shows an engineered flower-like actuator made by $Ti_3C_2T_x$–PP actuators.

Carbon nanocomposites can also be dispersed into ionic elastomers to create tunable stiffness and increased ionic conductivity [107,202]. A 3D macropore network [203] interpenetrated with a CNT-enriched conductive elastomer was fabricated to enhance the ionic conductivity up to almost 2×10^{-2} $S\cdot cm^{-1}$ and the bending angle up to 80° in 375 $V\cdot m^{-1}$ electric fields for underwater actuators.

Due to the low cost, flexibility, transparency, and light weight of the nano-carbon materials, IPCN actuators have potential applications in biomimetic microrobots, diaphragm-type micropumps, active micro-catheters, tactile displays, braille displays, and moving lenses [204]. Table 3 [16,103,128,199,201] summarizes the most important properties of IPCN actuators. Table 4 summarizes the advantages and disadvantages of the three classes of ionic elastomer actuators.

2.5. Perspectives for ionic elastomers for electromechanical actuators

Ionic elastomeric soft actuators have desirable applications in soft robotics, biomedical engineering, micro-manipulators, flow control, and so forth [146,205,206]. The current ionic elastomer actuators are limited by their slow response, weak actuation, need for patterned electrodes in order to achieve complex shapes, and lack of multifunctionality. Solving these problems not only requires novel smart-structured materials, but also advanced manufacturing technologies, programmable controls, and engineering designs.

Although the integration of independent electrode circuits is challenging for ionic elastomer actuators, the emergent 3D printing technology has provided a new approach for the manufacturing of soft materials with complex structures and high resolution that can enable rapid prototyping, customized design, and one-step production [160]. 3D printed structures with stimuli-responsive actuation over time as a new dimension are called 4D printed actuators [207]. With precise engineering designs and mathematical modeling, multiaxial actuations with designed routes and tasks can be programmed according to the reacting parameters [208]. 4D printed actuators integrated with 3D printed sensors can adjust their deformation by means of a controller and modeling system
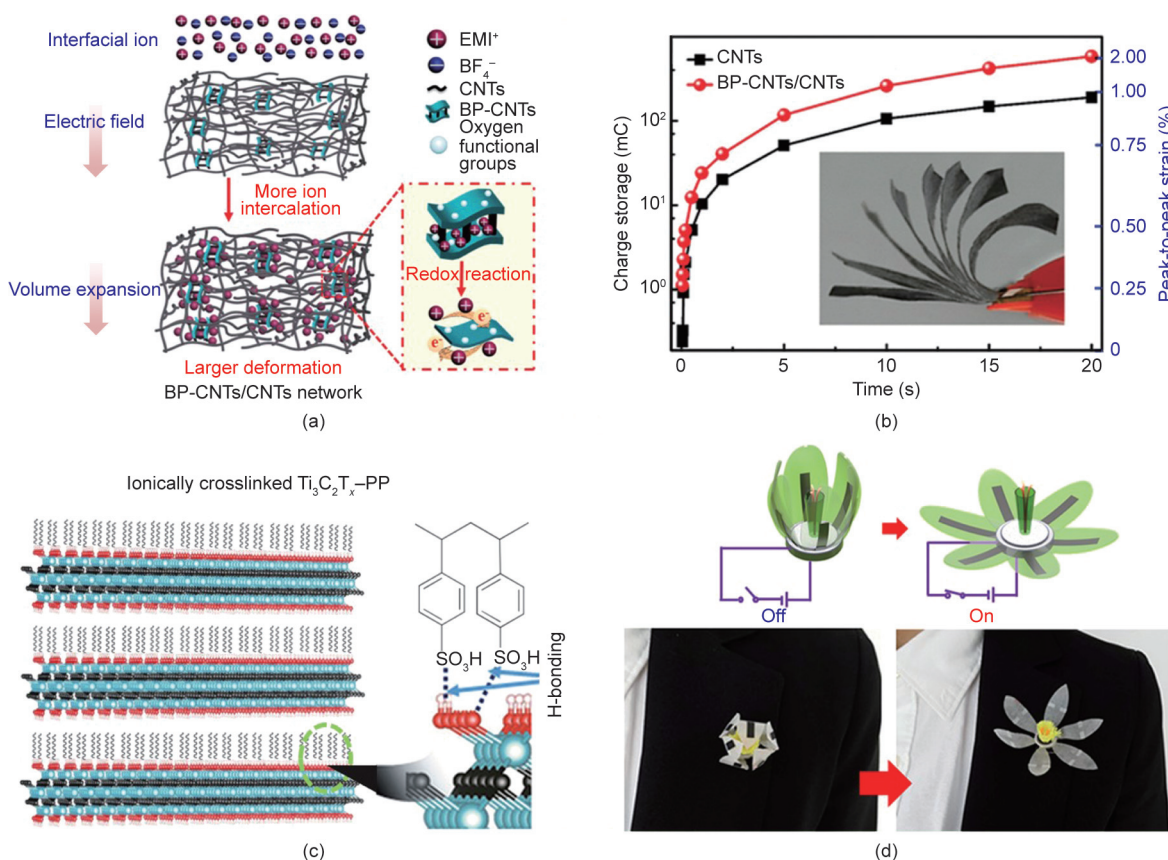
Fig. 6. Ionic elastomer actuator with hierarchical nano-structured carbon electrodes. (a) Schematics of the structure and ion transport inside a BP-based CNT electrode. (b) Time dependence of the actuation strain under 2.5 V and charge storage capacity with overlayed images of bending strips in the inset. (c) Layered structure of ionically crosslinked $Ti_3C_2T_x$–PP electrode. (d) Actuating flower engineering with $Ti_3C_2T_x$–PP actuators and wires. (a, b) Reproduced from Ref. [199] with permission of Wiley-VCH Verlag GmbH & Co. KGaA, ©2019; (c, d) reproduced from Ref. [201] with permission of the authors.

that can learn stimuli-responsive functions; thus, an adaptive 4D printed system can be achieved, as shown in Fig. 7(a) [209].

Self-sensing and multi-responsive ionic elastomer actuators that offer real-time feedback of motion, curvature, humidity, light, and temperature [210,211] are promising candidates for environmentally controlled self-adaptive robots. For example, ionic elastomer actuators with light weight, soft deformations, and low power consumption have future applications in aerospace—specifically, in aircraft wing morphing controlled by humans and the environment, as illustrated in Fig. 7(b) [212,213]. In addition, ionic elastomers with high capacity can be self-powered and wirelessly controlled in future soft robotic operations. For soft wearable robots, human-activity-involved interaction can be quantitively

evaluated and programmed in order to assist and mimic human behaviors by combining smart ionic elastomer actuators with machine learning (Fig. 7(c)) [214]. In the future, biocompatible ionic elastomer actuators can be used in microscopic biomedical robots for drug delivery, surgery, diagnostic imaging, and cardiac-assistance devices [215].

Motivated by the low voltage bending actuation of ionic elastomer actuators, IL of 1-hexyl-3-methylimidazolium (HMIM)-PF_6 with different size and/or mobility of positive and negative ions were incorporated into LCE networks photopolymerized by 4-(6-acryloxy-hex-1-yl-oxy)phenyl-4-(hexyloxy)benzoate (M1) and 1,4-bis-[4-(6-acryloyloxyhexyloxy)benzoyloxy]-2-methylbenzene) (M2) (Figs. 1(o) an (p)) in order to achieve the first iLCEs [73]. It

Table 3
Summary of performances of selected IPCN actuators.

Elastomer	PVDF-*co*-HFP	PSS-*b*-PMB/ZImS	PVDF-*co*-HFP	Nafion	PVDF-*co*-HFP
Electrode	SWCNT/PVDF-*co*-HFP	SWCNT	BP-CNTs	$Ti_3C_2T_x$–PP	Graphene/SWCNT
Cation	EMI^+, BMI^+, HMI^+, OMI^+	Imidazolium$^+$	EMI^+	EMI^+	EMI^+
Anion	BF_4^-	Polymerized SO_3^-	BF_4^-	BF_4^-	$TFSI^-$
Voltage (V)	2.0	3.0	2.5	1.0	2.0
Strain (%)	0.48, 0.45, 0.48, 0.60	0.90	1.00	0.68	0.91
Blocking force	NR	0.3 mN at 1 V	6 mN	4.71 mN	0.2g (g = 9.8 m·s^{-1})
Response time (ms)	100	100	50	50	10
Durability (cycles)	NR	20 000	500 000	18 000	NR
Back relaxation	No	No	No	No	No
Elastic modulus (MPa)	NR	NR	246	667	310
Reference	[128]	[16]	[199]	[201]	[103]

Table 4
Summary of the advantages and disadvantages of the three classes of ionic elastomer actuators.

| Ionic elastomer actuators	Advantages	Disadvantages
IPMCs	Good underwater operations (fast response, large strain and stress)	Unstable in air/dry conditions (electrode corrosion, slow response)
ICPs	Compliant elastic properties, sensing abilities, multiaxial shape changes, stable performance in air and water	Slow response, small bending strain, weak bending force
IPCNs	Fast response, stable in air/dry performance, large strain, low cost, biocompatible, transparent, micro-sizable	Weak bending force
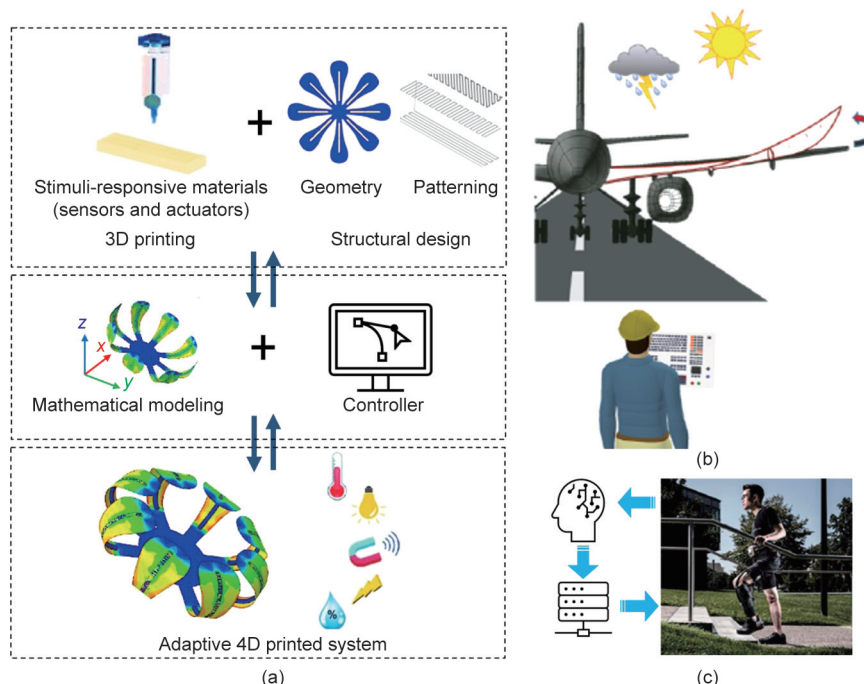
Fig. 7. Future processing and applications of ionic elastomer actuators. (a) Design concept of adaptive 4D printed soft robots combining sensing and actuating functions. (b) Future design of smart actuators in aircraft wing morphing for both human and environmental control. (c) Artificial intelligence actuators assisting human activities. (a) Reproduced from Ref. [209] with permission of the authors, ©2020; (b) reproduced from Ref. [212] with permission of the authors, ©2020; (c) reproduced from Ref. [214] with permission of Nature; ©2018.

was demonstrated that the iLCE could be actuated by even less than 1 V, with a bending strain comparable to that of the well-developed iEAPs. Furthermore, iLCEs exhibited several novel and superior features, such as dependence of the actuation on the alignment (Fig. 8) of the director of the LC. By spatially varying the alignment of anisotropic LCEs, the orientation and magnitude of the resulting strains can be easily preprogrammed and precisely controlled for soft robotic devices. Nematic LCEs with hybrid alignments (i.e., the director is parallel to the surface at one substrate and perpendicular at the other) are thermally active, and large bending curvatures have been achieved due to anisotropic thermal expansion coefficients on two sides of the film [21,216,217]. Therefore, hybrid iLCEs offer dual (thermal and electric) actuations. The multi-responsiveness of LC materials (e.g., magnetic field and light response) also offers interesting new applications compared with the current ionic elastomers.

3. Ionic elastomers for electromechanical sensors

Electromechanical sensors convert mechanical deformations into a measurable electrical quantity such as current, voltage, resistance, or capacitance. The mechanical deformation can be uniform strain (compression and/or dilation), which can be described

mathematically as $S_i = \Delta l_i / l_i = $ const (where l_i is the length of the material in one direction and Δl_i is its change), or can be non-uniform strain with a strain gradient $dS_i / dx_i \neq 0$. Bending deformation due to flexing is a special case of non-uniform strain. Electromechanical sensors can be made from carbon-based materials [218–220] (carbon grease, CNTs, graphene sheets), liquid metals [221,222], metals [223], metal nanowires/particles [224–229], and polymers [230–232]. Electromechanical bending sensors are widely used and are essential for many robotics applications [233] and for goniometric gloves [234]; they are also envisioned for artificial skin applications [235]. Today's bending sensors can respond to strain with changing resistance [236,237] or capacitance [238], or by producing flexoelectric and flexo-ionic current.

Most of the strain and pressure sensors based on ionic elastomers are resistive, capacitive, or flexo-ionic. The resistive technique uses the measurement of the electric resistance: $R = \rho l / A$, where R, ρ, l, and A are the resistance, resistivity, length, and cross-sectional area of the medium, respectively. When a mechanical deformation occurs, any of these quantities (ρ, l, A)—or all of them—may vary, resulting in a change in the resistance (Fig. 9(a)). The sensitivity or so-called gauge factor (GF) of the sensor is defined as $GF = \Delta R / (\varepsilon R_0)$, where ΔR, R_0, and ε are the relative change in resistance, the initial (deformed state) resistance, and the strain,
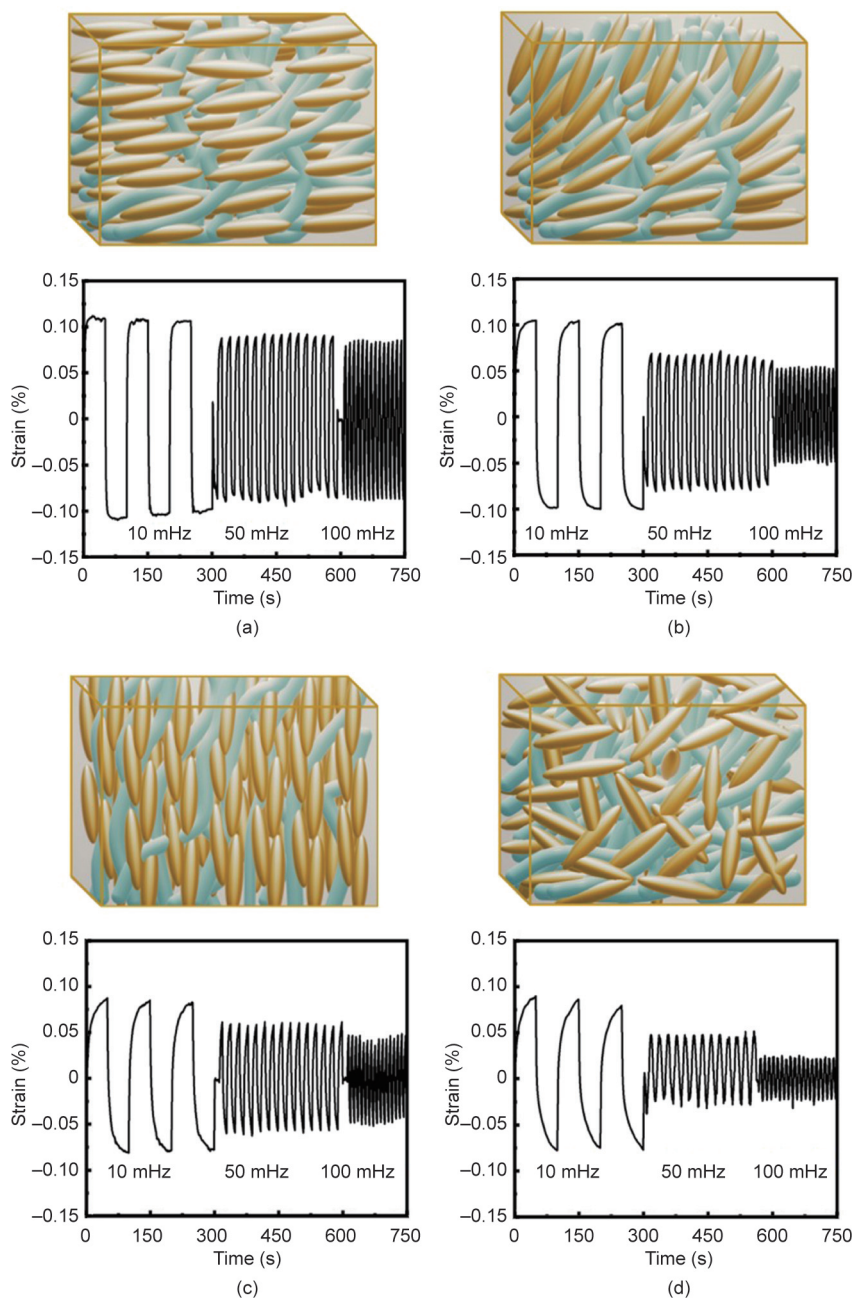
Fig. 8. Demonstration of the molecular alignment and bending performance of iLCEs with (a) planar, (b) hybrid, (c) homeotropic, and (d) isotropic alignments. Reproduced from Ref. [73] with permission of Wiley-VCH Verlag GmbH & Co. KGaA, ©2019.

respectively. In the case of resistive-type sensors, a low-voltage alternating current (AC) signal is used to measure the impedance instead of using simple DC resistance measurements, in order to avoid electrochemical reactions [239].

Although most stretching-based ionic elastomer strain sensors are resistive due to their reliability, simple construction, and easy measurement techniques [84,240], capacitive-type ionic elastomer strain sensors have also been reported occasionally. Capacitive sensors usually have lower humidity and temperature dependences [240–243]. They are composed of a dielectric material sandwiched between two electrodes. The basic functionality of a capacitive-type sensor is a variation of the capacitance, $C = \varepsilon_0 \varepsilon_r A / d$ (where ε_0, ε_r, A, and d are the dielectric constant of a vacuum, the relative dielectric constant, the cross-sectional area, and the thickness of the dielectric layer, respectively), due to a change in any of these parameters (ε_r, A, d) resulting from uniform strain/pressure. The gauge factor for a capacitive-type sensor is given as $GF = \Delta C / (\varepsilon C_0)$, where the ΔC, C_0, and ε are relative change in capacitance, initial (deformed state) capacitance, and strain (Fig. 9(b)). Another important term in sensor technology is hysteresis, which denotes repeatability. To quantitatively compare the magnitude of the hysteresis, the degree of hysteresis (DH) [45] is defined as $DH = (A_S - A_R) / A_S \times 100\%$, where A_S and A_R are the area of the stretching and releasing state curve, respectively, in a relative resistance (capacitance) versus strain graph. The advantages of capacitive-type sensors are their high sensitivity, lower hysteresis, and low power consumption [80,244–246]. On the other hand, resistive-type sensors have the advantages of easy fabrication, low cost, easy signal acquisition, and a wide detection range [244,247,248].

The detection of bending deformations with ionic elastomers is often based on flexo-ionic effects [70,249–251], whereby differently sized cations (usually larger) and anions (usually smal-
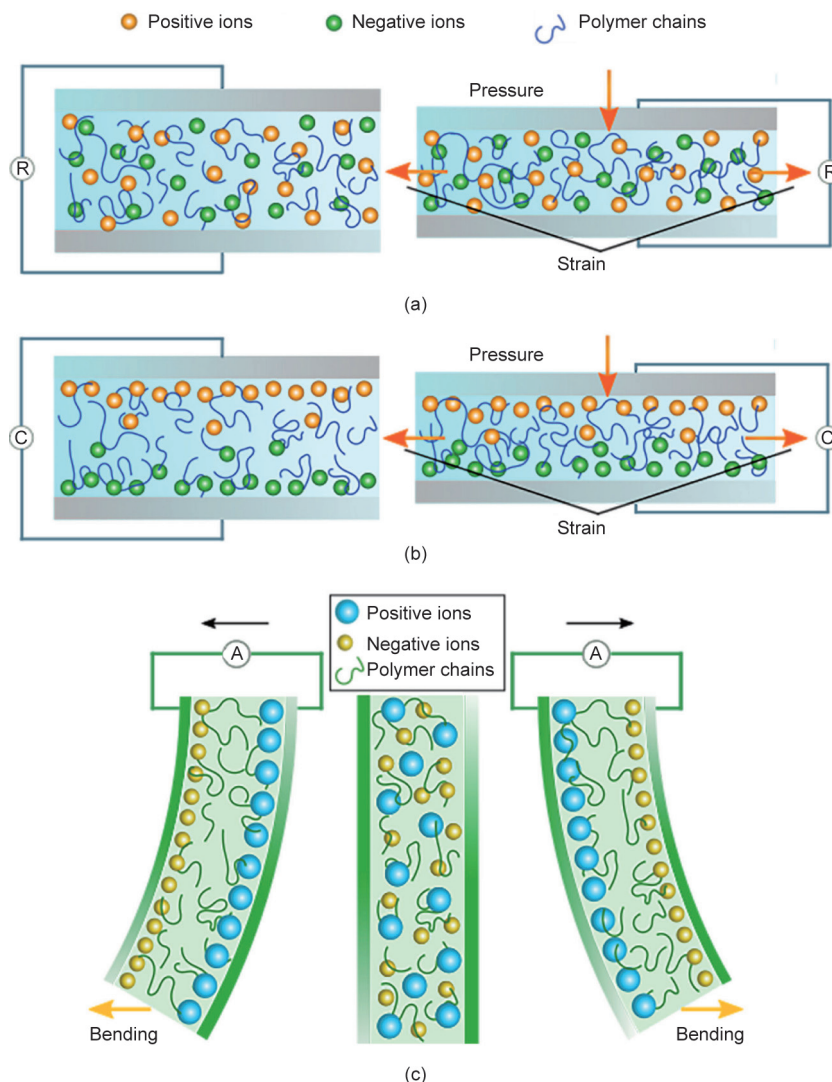
Fig. 9. Schematic illustration of the transduction mechanism of ionic elastomer sensors. (a) Resistive-type sensors are based on the change in resistance upon applying pressure or strain. (b) In capacitive-type sensors, the capacitance is changed upon the application of pressure and strain. (c) Illustration of voltage (current) generation upon bending due to the separation of differently sized ions.

ler) are used inside an elastomeric (e.g., poly(ethylene glycol) diacrylate (PEGDA)) matrix. Upon bending the polymer film, cations and anions are forced to separate due to the volumetric asymmetry in the anode and cathode, creating a potential difference, as illustrated in Fig. 9(c). This effect is the inverse of the bending actuation based on different sized ions, which was described in Section 2. The bending-induced electric current or voltage is proportional to the bending angle. This method is sensitive to the bending direction, which is a major advantage of these sensors. In addition, such devices can be developed for micropower generation [71,252].

Ionic elastomers are rarely explored as shear sensors [253,254], and most of the research on sensing has focused on uniform strains and bending strain sensing.

Fig. 10 lists the elastomers and ILs that are most often used for ionic elastomer sensors and are not already listed as actuator materials in Fig. 1.

3.1. Strain sensors

A large variety of elastomeric materials, ionic entities, and fabrication methods have been proposed in order to develop ionic strain sensors for various applications. Xie et al. [255] have demonstrated the hierarchical self-assembly of functionalized Pluronic block-copolymers mixed with IL ethyl ammonium nitrate (EAN) into a face-centered cubic structure, as shown in Fig. 11(a). The long polymer chains connecting the self-assembled micelles result in high stretchability (breakage at 3000% strain), good cyclability, and a linear relationship with resistance and strain [255,256]. Small-angle X-ray scattering (SAXS) shows two-stage microstructure transition (Fig. 11(b)) [256] during uniaxial elongation. Importantly, these sensors do not suffer from microscopic cracks and breakages, which makes them highly durable [220,257,258].

Conductive hydrogels (often called "ionic hydrogels") and ionogels are other classes of soft elastic materials, which are used in sensor fabrication due to their unique properties. Conductive hydrogels are water-swollen polymer networks with conductive fillers [259] (mostly solvated salts [260,261]), while ionogels are polymer matrices mixed with ILs [262–267]. Most hydrogels and ionogels are biocompatible and can be made softer than tissues, which is important in soft sensors in order to avoid constraining body motions. Ionogels are nonvolatile and are more suitable for open-air applications than hydrogels, which tend to dry out in open air due to water evaporation. To restrain the dehydration of
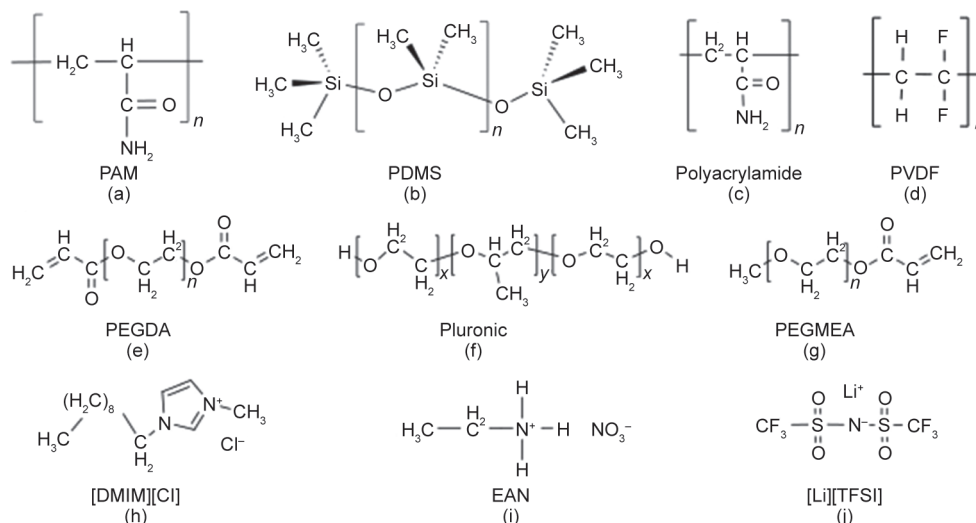
Fig. 10. Molecular structures of widely used (a–g) elastomers and (h–j) ILs in electromechanical sensing. PAM: polyacrylamide; PDMS: polydimethylsiloxane; PEGMEA: poly(ethylene glycol)methyl ether acrylate; [DMIM][Cl]: 1-decyl 3-methyl imidazolium chloride; EAN: ethyl ammonium nitrate; [Li][TFSI]: lithium bis(trifluoromethane-sulfonyl) imide.
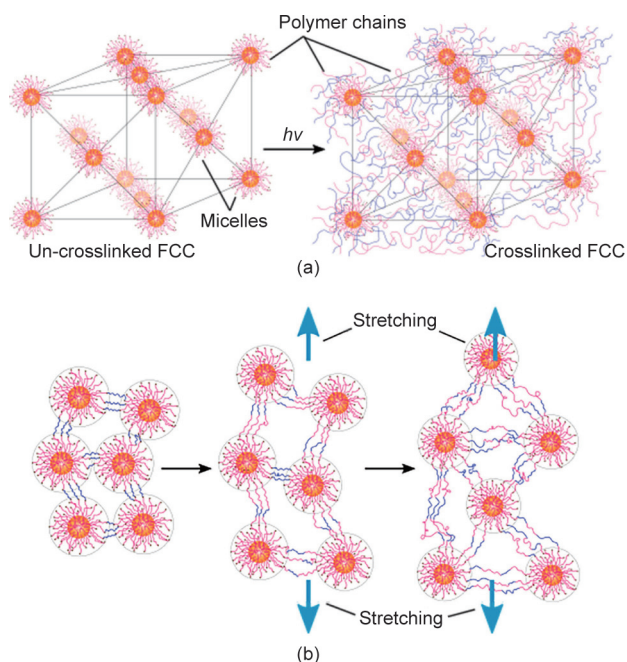

Fig. 11. Illustration of a Pluronic block-copolymer structure and sensing mechanism. (a) Self-assembled face-centered cubic (FCC) structure in the presence of IL EAN. (b) Two-stage microstructure transition upon uniaxial elongation. (a) Reproduced from Ref. [255] with permission of National Academy of Inventors, ©2018; (b) reproduced from Ref. [256] with permission of American Chemical Society, ©2018.

a hydrogel, polydimethylsiloxane (PDMS) encapsulation is used extensively. Polyacrylamide (PAM) is a widely used elastomeric material for hydrogel-based strain sensors [51,78,91]. Hygroscopic salts (mostly LiCl and NaCl) are used for conductive elements, since they help the stability of the hydrogels by absorbing water and keeping the relative humidity constant [78]. Gu et al. [51] developed a highly stretchable (~300% strain) and transparent (~95% transmittance in the visible light range) hydrogel elastomer ionic sensor that not only monitored finger motion, but also recognized hand gestures and sign language.

Ionogel (rGO dispersed in IL)-based 3D printed strain sensors have achieved a 350% strain range, less than 3.5% of degree of hysteresis, and good reproducibility (5000 cycles) [268]. The inclusion of rGO increases the conductivity by 45%, and hence boosts the sensitivity. Stencil-printed electrodes using silver flake/Ecoflex paste reduce the constraint to the flexibility of the system. Table 5 [51,70,71,77,78,81,91,239,252,255,256,268,269] summarizes the most important properties of the most widely known strain sensors along with some additional information, such as fabrication techniques.

3.2. Pressure sensors

Pressure sensing is vital in many applications, such as in diagnosing heart failures, respiratory disorders, cardiovascular diseases, and sports injuries [4]. Different parts of the human body generate various levels of pressure during different physical activities. Intra-body pressures such as intraocular and intracranial pressures are low pressures (< 10 kPa) [4]. Medium pressures (< 100 kPa) are generated by the heart, jugular venous pulses, blood pressure, and so forth [4,270]. The pressures exerted on a foot by body weight and large-scale body motion can be considered to be high pressures (> 100 kPa) [4,270]. To monitor these various ranges of pressure, highly sensitive and stretchable pressure sensors are required. In addition to patterned microstructures [271,272], porous structures [273,274], nanomaterials [275,276], and ionic elastomers are suitable as sensitive pressure sensors.

Solvent-free ionic elastomer materials show great potential in wearable electronics, since they are stable in ambient air and maintain the original stretchability, transparency, and conductivity with time, due to negligible weight loss or decay [277]. Various research groups have developed solvent-free IL or ionic salt polymer composites for pressure sensing [277–280]. Shi et al. [277] demonstrated a very stable (to air, temperature, adhesion, and voltage) ionic conductive elastomer consisting of LiTFSI, PEGDA, and butyl acrylate (BA). The electrolyte and metal electrode interfaces were found to be much less corrosive than hydrogel–metal interfaces. Furthermore, the inclusion of comonomers into the system enhanced the conductivity and hence increased the sensitivity of the pressure sensor. The degree of polymerization and crosslinking, the concentration of ionic entity, and the dimensions of the

Table 5
Basic properties of selected strain sensors.

Materials	Ionic entity	Strain range (%)	Sensitivity (gauge factor)	Additional information
Butyl acrylate (CNT mixed) [81]	Acrylic acid, dimethylaminoethyl methacrylate	< 250	431.30 (50%–58% strain)	Self-healing (> 80% strain)
PAM/PDMS [78]	LiCl	< 50	0.84 (up to 40%)	Hydrogel/3D printable
Polyetheramine, PEGDA [239]	NaCl	< 30	2 (< 30% strain)	Ionic hydrogel
PDMS [268]	[BMI][BF$_4$]/rGO	< 350	0.54–2.41	Ionogel/3D printable
Styrene-butadiene rubber/carbon black [269]	[DMIM][Cl]	~40–180	NR	NR
Pluronic [255,256]	EAN	< 340	0.01–1	Block-copolymer
PEGDA [77]	Acrylic acid, choline chloride	< 150	NR	3D patternable
PAM, PDMS (for encapsulation) [51]	LiCl	~300	~0.8	Hydrogel
PAM, acrylic elastomer [91]	NaCl	1–500	NR	Ionic hydrogel
PEGDA/TS [70]	[HMIM][PF$_6$]	< 50	NR	Flexo-ionic principle
PEGDA/SCN [71]	[Li][TFSI]	< 50	NR	Flexo-ionic principle
PEGDA/PEGMEA [252]	[Li][TFSI]	< 50	NR	Flexo-ionic principle

active material greatly affected the sensitivity of the sensor [278,279].

In addition to the application of ionic hydrogels in strain sensing, ionic hydrogels are used in pressure sensing [82,267,281,282]. Enriching the sensitivity and mechanical properties, ultra-stretchable (1500%) ionic hydrogels have been developed by Darabi et al. [82]. PPA-based hydrogel and ferric ions are being used to fabricate an ionic elastomeric pressure sensor that can measure pressures from 0 to 0.45 kPa, which is suitable for intra-body pressure measurements. The repeated compression response to different elongations (25% and 50% strain) shows the versatility of this sensor. Using pneumatic tubes with hydrogel skins, the sensor can measure pneumatic pressures as well as compression pressures, such as a finger press [267]. Due to their optical transparency and stretchability, ionic hydrogels are often used for the electrodes of the sensor as well [282].

Microstructure, such as intermediate ridges (Fig. 12(a)), is essential in human skin in order to enhance the sensitivity under mechanical stimulus [94]. The microstructure of human skin has inspired several studies on ionic elastomeric pressure sensors

[90,283–285]. Micropatterning enables ultrasensitive pressure detection with a fast response time and low power consumption. Different microstructure shapes, such as the pyramid shape [90,285], cone-shape [283], and spherical cap shape [284], have been constructed. When these topographically patterned ionic elastomers (mostly ionic gels) are sandwiched between two electrodes, periodic air gaps are created. When a pressure is applied, these air gaps decrease, resulting in a large increase of the effective capacitance of the sensor, leading to ultra-sensitiveness. PVDF-*co*-HFP gel mixed with EMI-TFSI (Fig. 1(e)) IL is a widely used sensing material for micropatterned pressure sensors, due to its high capacitance and high tensile strength. A comparison of the sensitivity with and without microstructures has been done by Cho et al. [285]. A flat ion gel-based pressure sensor has an order of magnitude higher specific capacitance than a pyramidal shape micropatterned pressure sensor, where the capacitance can be significantly controlled by the applied pressure, making the pressure sensor highly sensitive. Having randomly distributed different sizes of microstructures enhances the sensitivity further [284].
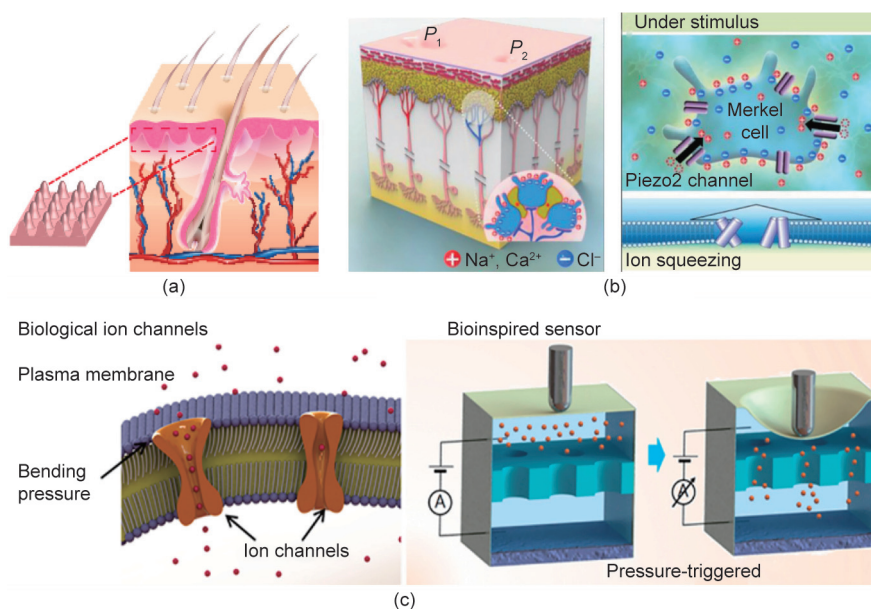

Fig. 12. Bio-inspired sensing. (a) Human skin and intermediate ridges (inset). (b) Mechanism of pressure sensing by the skin by squeezing ions into Merkel cells via piezo channels (P_1 and P_2 are two points activated with two different magnitudes of pressures). (c) Representation of biological cells with ion channels that are sensitive to bending pressure (left) and a sketch of a bio-inspired pressure sensor (right). (b) Reproduced from Ref. [286] with permission of Wiley-VCH Verlag GmbH & Co. KGaA, ©2017; (c) reproduced from Ref. [287] with permission of the American Chemical Society, ©2016.

In addition to the detection of compression force, sensing shear forces and torsions are achieved by a unique microstructure called a pyramid-plug structure [90]. The fabrication of these microstructures requires expensive lithographic techniques. To address this issue, Qiu et al. [283] reported a microstructure templated from a *Calathea zebrine* leaf using soft lithography.

Pressure sensors, which are inspired by ion transportation through nano-porous ion channels in cell membranes, have been developed with high sensitivity and stability in a wide pressure range [286,287]. The Piezo2 protein, which contains mechanically activated ion nano-channels, performs the mechano-transduction of the Merkel cells [288,289], as illustrated in Fig. 12(b). Adopting this mechanism, Jin et al. [286] developed an advanced pressure sensor. They demonstrated the sensing of extremely low pressures (10–100 Pa), such as the pressure a goose feather imposes on a surface, the sound pressure of a whisper, or the pressure of artery pressure waves. The ion channels of biological plasma membranes have inspired pressure sensors that show a very low response time (~12 ms) [287]. Recently, skin-inspired (Fig. 12(c)) ionic elastomer-based pressure sensors, in which the sensing mechanism is based on ion transportation under external stimuli, have gained a great deal of attention due to their unique biocompatibility.

The material properties, fabrication techniques, and performances of various resistive and capacitive ionic elastomeric pressure sensors are tabulated in Table 6 [90,261,267,282–287] and Table 7 [82,90,277–281], respectively.

3.3. Future possibilities

Over the past few decades, there has been flourishing development of soft robotics, inspired by mimicking the actuation of soft structures in nature [214,290–294]. Unlike traditional hard robots, which have limited degrees of freedom in discrete motions, soft robots using stimuli-responsive resilient materials can generate an infinite number of continuous shape deformations without damaging their payloads [295–297]. Compliant elasticity, good adaptability to external constraints, and safety around humans render soft robotics potentially useful in healthcare and artificial intelligence [298–300]. Soft robotic applications require the development of soft materials that are resilient and elastic, and can therefore perform repeated actuation and sensing after many cycles.

In spite of the significant progress that has been made over the past decade, ionic elastomeric electromechanical sensors are in their early stage, and significant challenges remain; thus, they require further development. Novel materials and different fabrication processes can play an important role in addressing the remaining challenges, such as improving the accuracy, power consumption, sensitivity, reliability, compatibility, and repeatability. As described in the section above, surface microstructures and bio-inspired ion-channel-based elastomers could enhance sensor performance.

High sensitivity, stretchability, durability, and accuracy, along with a fast response, biocompatibility, and low cost, are the requirements of future wearable strain sensors in the applications of biomechanical capturing, sports performance tracking, feedbacks from soft robotics, and rehabilitation monitoring [4,51,256,301–303]. In these applications, the simultaneous detection of large-scale motions (e.g., stretching, torsion, and bending movements of hands, legs, neck, fingers, spinal) and small-scale motions (e.g., heartbeat, pulse, facial expressions, breathing, swallowing, eye blinking, and speaking) is needed [80,304–306].

We consider that designing an inner elastomer structure with spatially varying configurations may open doors for more diverse electromechanical sensors. For this purpose, iLCEs with different structures (i.e., planar, hybrid, homeotropic, and isotropic), as depicted in Figs. 8(a)–(d), have great potential. Flexo-ionic polarization (the converse effect of the electro-actuation shown in Fig. 8) is shown at the function of the bending curvature in Fig. 13(a). Similar to electro-actuation, flexo-polarization strongly depends on the structure that can be preprogrammed at the crosslinking stage. The flexo-ionic coefficients (the slope of the polarization vs curvature graph) obtained from iLCEs are comparable to those of the well-developed electroactive polymers (EAPs) [70,71,252]. Moreover, iLCEs offer an additional degree of freedom to tune the sensitivity of the device. Nevertheless, the low output current (microampere level) requires advanced current-

Table 6
Basic properties of capacitive-type pressure sensors. Some unique material and structural properties of the sensors are listed in the last column.

Materials	Ionic entity	Pressure range (kPa)	Sensitivity (kPa^{-1})	Additional information
PAM [261]	ZnS	0–30	—	Electroluminescent
PDMS/PAM [282]	NaCl	0–250	0.011	Hydrogel electrodes
PAM/silicone [267]	[DMIM][Cl]	10–65.5	—	Hydrogel/3D printable
P(VDF-HFP) [283]	[EMI][TFSI]	0.001–115	~54	Cone-shape microstructure
TPU [90]	[EMI][TFSI]	0–10	0.7	Pyramid shape microstructure
		10–50	0.1	
P(VDF-HFP) [284]	[EMI][TFSI]	< 2	~131	Randomly distributed microstructure
P(VDF-HFP) [285]	[EMI][TFSA]	< 50	41	Pyramid shape microstructure
TPU [286]	[EMI][TFSI]	10–100	25.8	Ionic nano-channels
Silicone/PVDF [287]	PANI solution	10–20	5.6	Ionic nano-channels

P(VDF-HFP): poly(vinylidene fluoride-*co*-hexafluoropropylene); TFSA: bis(trifluoromethylsulfonyl)amide.

Table 7
Basic properties of resistive-type pressure sensors. Some unique material and structural properties of the sensors are listed in the last column.

Materials	Ionic entity	Pressure range (kPa)	Sensitivity (gauge factor)	Additional information
BACOEA [278]	[EMI][BF$_4$]	—	~0.45	3D printable
TangoPlus [279,280]	[EMI][BF$_4$]	0–15	~1.5	3D printable/CNT based electrodes
Acrylamide [281]	LiCl	90–230	~2010 MPa^{-1}	Hydrogel/3D printable
PPy [82]	Ferric ions	0–0.45	—	Hydrogel/3D printable
PEGDA/BA [277]	[Li][TFSI]	—	—	—
TPU [90]	[EMI][TFSI]	0–10	0.7 kPa^{-1}	Pyramid shape microstructure
		10–50	0.1 kPa^{-1}	

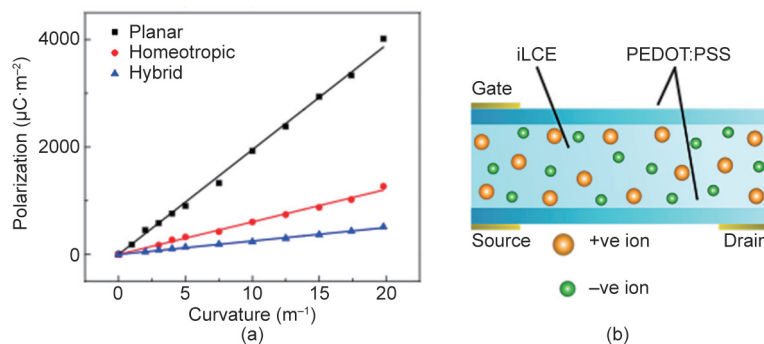BACOEA: 2-[[(butylamino)carbonyl]oxy]ethyl acrylate.

Fig. 13. Preliminary results showing the potential of using iLCEs in various alignments (planar, homeotropic, and hybrid). (a) Flexo-ionic polarization at the function of bending curvature. (b) Schematic diagram of an OECT based on of iLCEs.

measuring techniques, such as lock-in amplifiers. Signals can be considerably amplified and an advanced bending sensor can be obtained by integrating iLCEs into an OECT, as shown in Fig. 13(b). When bending takes place, the device drives ions into the PEDOT:PSS layer in between the source and drain electrodes. This modulates the conductivity of this layer; hence, the current flows from the source to the drain. Preliminary results have demonstrated the feasibility of this principle. An iLCE can also be used as the gate electrolyte, which provides an additional degree of freedom to optimize the system through different alignments. The high sensitivity obtained by combining iEAPs and iLCEs with OECTs to amplify the flexo-ionic current opens a new window in the field of strain sensors. This sensor can be easily combined with other sensing mechanisms, such as electrochemical and gas sensing, which is a major requirement in wearable devices.

4. Summary

In this paper, we reviewed recent developments in the ionic elastomers used as sensors and actuators. This summary of recent results and our discussion of the perspectives clearly indicate that future actuators and sensors not only have to work together, but must also be adaptive by varying their properties based on past actuations and sensing experiences. These complex systems will be functional for longer time scales and may even be self-

repairable. Such synergy is illustrated in Fig. 14, which also serves as a graphical abstract for this paper by summarizing the essence of the latest and future ionic elastomer actuators and sensors that will be integrated into future soft robots.

Compliance with ethics guidelines

Chenrun Feng, C.P. Hemantha Rajapaksha, and Antal Jákli declare that they have no conflict of interest or financial conflicts to disclose.
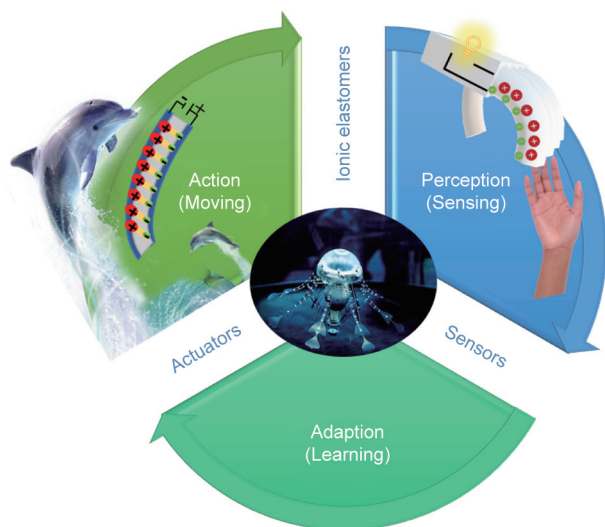

Fig. 14. Illustration of the synergy of future actuators and sensors, which will not only have to work together in soft robotics, but must also be adaptive by varying their properties based on past actuations and sensing experiences.

References

[1] Bandodkar AJ, Wang J. Non-invasive wearable electrochemical sensors: a review. Trends Biotechnol 2014;32(7):363–71.
[2] Pang C, Lee C, Suh KY. Recent advances in flexible sensors for wearable and implantable devices. J Appl Polym Sci 2013;130(3):1429–41.
[3] Amjadi M, Kyung KU, Park I, Sitti M. Stretchable, skin-mountable, and wearable strain sensors and their potential applications: a review. Adv Funct Mater 2016;26(11):1678–98.
[4] Trung TQ, Lee NE. Flexible and stretchable physical sensor integrated platforms for wearable human-activity monitoring and personal healthcare. Adv Mater 2016;28(22):4338–72.
[5] Majumder S, Mondal T, Deen MJ. Wearable sensors for remote health monitoring. Sensors 2017;17(1):130.
[6] Yang T, Xie D, Li Z, Zhu H. Recent advances in wearable tactile sensors: materials, sensing mechanisms, and device performance. Mater Sci Eng Rep 2017;115:1–37.
[7] Haddara YM, Howlader MMR. Integration of heterogeneous materials for wearable sensors. Polymers 2018;10(1):60.
[8] Heikenfeld J, Jajack A, Rogers J, Gutruf P, Tian L, Pan T, et al. Wearable sensors: modalities, challenges, and prospects. Lab Chip 2018;18(2):217–48.
[9] Liu Y, Wang H, Zhao W, Zhang M, Qin H, Xie Y. Flexible, stretchable sensors for wearable health monitoring: sensing mechanisms, materials, fabrication strategies and features. Sensors 2018;18(2):645.
[10] Lim HR, Kim HS, Qazi R, Kwon YT, Jeong JW, Yeo WH. Advanced soft materials, sensor integrations, and applications of wearable flexible hybrid electronics in healthcare, energy, and environment. Adv Mater 2020;32(15):1901924.
[11] Bar-Cohen Y, editor. Electroactive polymer (EAP) actuators as artificial muscles: reality, potential, and challenges. Washington, DC: SPIE Press; 2004.
[12] Kim KJ, Tadokoro S. Electroactive polymers for robotic applications: artificial muscles and sensors. London: Springer; 2007.
[13] Sugawara E, Nikaido H. Properties of AdeABC and AdeIJK efflux systems of *Acinetobacter baumannii* compared with those of the AcrAB-TolC system of *Escherichia coli*. Antimicrob Agents Chemother 2014;58(12):7250–7.
[14] Kim O, Shin TJ, Park MJ. Fast low-voltage electroactive actuators using nanostructured polymer electrolytes. Nat Commun 2013;4(1):2208.
[15] Kim O, Kim SJ, Park MJ. Low-voltage-driven soft actuators. Chem Commun 2018;54(39):4895–904.
[16] Kim O, Kim H, Choi UH, Park MJ. One-volt-driven superfast polymer actuators based on single-ion conductors. Nat Commun 2016;7(1):13576.
[17] Kim SJ, Kim O, Park MJ. True low-power self-locking soft actuators. Adv Mater 2018;30(12):1706547.

[18] Hu W, Zhao H, Song L, Yang Z, Cao H, Cheng Z, et al. Electrically controllable selective reflection of chiral nematic liquid crystal/chiral ionic liquid composites. Adv Mater 2010;22(4):468–72.

[19] Wang M, Zou C, Sun J, Zhang L, Wang L, Xiao J, et al. Asymmetric tunable photonic bandgaps in self-organized 3D nanostructure of polymer-stabilized blue phase I modulated by voltage polarity. Adv Funct Mater 2017;27(46):1702261.

[20] Hirai T. Magnetic fluid composite gels. In: Asaka K, Okuzaki H, editors. Soft actuators: materials, modeling, applications, and future perspectives. Singapore: Springer Singapore; 2019. p. 347–62.

[21] Shahsavan H, Salili SM, Jákli A, Zhao B. Thermally active liquid crystal network gripper mimicking the self-peeling of gecko toe pads. Adv Mater 2017;29(3):1604021.

[22] Wang L, Jian Y, Le X, Lu W, Ma C, Zhang J, et al. Actuating and memorizing bilayer hydrogels for a self-deformed shape memory function. Chem Commun 2018;54(10):1229–32.

[23] Zhang L, Desta I, Naumov P. Synergistic action of thermoresponsive and hygroresponsive elements elicits rapid and directional response of a bilayer actuator. Chem Commun 2016;52(35):5920–3.

[24] Ilievski F, Mazzeo AD, Shepherd RF, Chen X, Whitesides GM. Soft robotics for chemists. Angew Chem Int Ed Engl 2011;50(8):1890–5.

[25] Moseley P, Florez JM, Sonar HA, Agarwal G, Curtin W, Paik J. Modeling, design, and development of soft pneumatic actuators with finite element method. Adv Eng Mater 2016;18(6):978–88.

[26] Zarzar LD, Kim P, Aizenberg J. Bio-inspired design of submerged hydrogel-actuated polymer microstructures operating in response to pH. Adv Mater 2011;23(12):1442–6.

[27] Yu C, Yuan P, Erickson EM, Daly CM, Rogers JA, Nuzzo RG. Oxygen reduction reaction induced pH-responsive chemo-mechanical hydrogel actuators. Soft Matter 2015;11(40):7953–9.

[28] Yoshino T, Kondo M, Mamiya J, Kinoshita M, Yu Y, Ikeda T. Three-dimensional photomobility of crosslinked azobenzene liquid-crystalline polymer fibers. Adv Mater 2010;22(12):1361–3.

[29] Han DD, Zhang YL, Ma JN, Liu YQ, Han B, Sun HB. Light-mediated manufacture and manipulation of actuators. Adv Mater 2016;28(38):8328–43.

[30] Wang L, Urbas AM, Li Q. Nature-inspired emerging chiral liquid crystal nanostructures: from molecular self-assembly to DNA mesophase and nanocolloids. Adv Mater 2020;32(41):1801335.

[31] Wang M, Zou C, Li C, Sun J, Wang L, Hu W, et al. Bias-polarity dependent bidirectional modulation of photonic bandgap in a nanoengineered 3D blue phase polymer scaffold for tunable laser application. Adv Opt Mater 2018;6(16):1800409.

[32] Wang L, Bisoyi HK, Zheng Z, Gutierrez-Cuevas KG, Singh G, Kumar S, et al. Stimuli-directed self-organized chiral superstructures for adaptive windows enabled by mesogen-functionalized graphene. Mater Today 2017;20(5):230–7.

[33] Ikeda T, Mamiya J, Yu Y. Photomechanics of liquid-crystalline elastomers and other polymers. Angew Chem Int Ed Engl 2007;46(4):506–28.

[34] Li MH, Keller P. Artificial muscles based on liquid crystal elastomers. Philos Trans A 1847;2006(364):2763–77.

[35] Jákli A. Electro-mechanical effects in liquid crystals. Liq Cryst 2010;37(6–7):825–37.

[36] Pelrine R, Kornbluh R, Joseph J, Heydt R, Pei Q, Chiba S. High-field deformation of elastomeric dielectrics for actuators. Mater Sci Eng C 2000;11(2):89–100.

[37] Romasanta LJ, Lopez-Manchado MA, Verdejo R. Increasing the performance of dielectric elastomer actuators: a review from the materials perspective. Prog Polym Sci 2015;51:188–211.

[38] Zhang QM, Bharti V, Zhao X. Giant electrostriction and relaxor ferroelectric behavior in electron-irradiated poly(vinylidene fluoride-trifluoroethylene) copolymer. Science 1998;280(5372):2101–4.

[39] Ohm C, Brehmer M, Zentel R. Liquid crystalline elastomers as actuators and sensors. Adv Mater 2010;22(31):3366–87.

[40] White TJ, Broer DJ. Programmable and adaptive mechanics with liquid crystal polymer networks and elastomers. Nat Mater 2015;14(11):1087–98.

[41] Mirfakhrai T, Madden JDW, Baughman RH. Polymer artificial muscles. Mater Today 2007;10(4):30–8.

[42] Hines L, Petersen K, Lum GZ, Sitti M. Soft actuators for small-scale robotics. Adv Mater 2017;29(13):1603483.

[43] Lehmann W, Skupin H, Tolksdorf C, Gebhard E, Zentel R, Krüger P, et al. Giant lateral electrostriction in ferroelectric liquid-crystalline elastomers. Nature 2001;410(6827):447–50.

[44] Bar-Cohen Y, Zhang Q. Electroactive polymer actuators and sensors. MRS Bull 2008;33(3):173–81.

[45] Yoon SG, Koo HJ, Chang ST. Highly stretchable and transparent microfluidic strain sensors for monitoring human body motions. ACS Appl Mater Interfaces 2015;7(49):27562–70.

[46] Chossat JB, Park YL, Wood RJ, Duchaine V. A soft strain sensor based on ionic and metal liquids. IEEE Sens J 2013;13(9):3405–14.

[47] Choi DY, Kim MH, Oh YS, Jung SH, Jung JH, Sung HJ, et al. Highly stretchable, hysteresis-free ionic liquid-based strain sensor for precise human motion monitoring. ACS Appl Mater Interfaces 2017;9(2):1770–80.

[48] Zhang SH, Wang FX, Li JJ, Peng HD, Yan JH, Pan GB. Wearable wide-range strain sensors based on ionic liquids and monitoring of human activities. Sensors 2017;17(11):2621.

[49] Wang H, Wang Z, Yang J, Xu C, Zhang Q, Peng Z. Ionic gels and their applications in stretchable electronics. Macromol Rapid Commun 2018;39(16):1800246.

[50] Yang C, Suo Z. Hydrogel ionotronics. Nat Rev Mater 2018;3(6):125–42.

[51] Gu G, Xu H, Peng S, Li L, Chen S, Lu T, et al. Integrated soft ionotronic skin with stretchable and transparent hydrogel–elastomer ionic sensors for hand-motion monitoring. Soft Robot 2019;6(3):368–76.

[52] Keulemans G, Pelgrims P, Bakula M, Ceyssens F, Puers R. An ionic liquid based strain sensor for large displacements. Procedia Eng 2014;87:1123–6.

[53] Antony P, De SK. Ionic thermoplastic elastomers: a review. J Macromol Sci Part C 2001;41(1–2):41–77.

[54] Soares BG. Ionic liquid: a smart approach for developing conducting polymer composites: a review. J Mol Liq 2018;262:8–18.

[55] Rajapaksha CPH, Feng C, Piedrahita C, Cao J, Kaphle V, Lüssem B, et al. Poly(ethylene glycol) diacrylate based electro-active ionic elastomer. Macromol Rapid Commun 2020;41(6):1900636.

[56] Feng C, Kyu T. Role of dinitrile plasticizer chain lengths in electrochemical performance of highly conductive polymer electrolyte membrane for lithium ion battery. Electrochim Acta 2020;330:135320.

[57] Hao M, Wang Y, Zhu Z, He Q, Zhu D, Luo M. A compact review of IPMC as soft actuator and sensor: current trends, challenges, and potential solutions from our recent work. Front Robot AI 2019;6:129.

[58] Anderson IA, Gisby TA, McKay TG, O'Brien BM, Calius EP. Multi-functional dielectric elastomer artificial muscles for soft and smart machines. J Appl Phys 2012;112(4):041101.

[59] Kurumaya S, Suzumori K, Nabae H, Wakimoto S. Musculoskeletal lower-limb robot driven by multifilament muscles. Robomech J 2016;3(1):18.

[60] Polygerinos P, Wang Z, Galloway KC, Wood RJ, Walsh CJ. Soft robotic glove for combined assistance and at-home rehabilitation. Rob Auton Syst 2015;73:135–43.

[61] Bauer S, Bauer-Gogonea S, Graz I, Kaltenbrunner M, Keplinger C, Schwödiauer R. 25th anniversary article: a soft future: from robots and sensor skin to energy harvesters. Adv Mater 2014;26(1):149–61.

[62] Kim S, Laschi C, Trimmer B. Soft robotics: a bioinspired evolution in robotics. Trends Biotechnol 2013;31(5):287–94.

[63] Wei D, Ivaska A. Applications of ionic liquids in electrochemical sensors. Anal Chim Acta 2008;607(2):126–35.

[64] Silvester DS. Recent advances in the use of ionic liquids for electrochemical sensing. Analyst 2011;136(23):4871–82.

[65] Ma Y, Pharr M, Wang L, Kim J, Liu Y, Xue Y, et al. Soft elastomers with ionic liquid-filled cavities as strain isolating substrates for wearable electronics. Small 2017;13(9):1602954.

[66] Singh VV, Nigam AK, Batra A, Boopathi M, Singh B, Vijayaraghavan R. Applications of ionic liquids in electrochemical sensors and biosensors. Int J Electrochem 2012;2012:165683.

[67] Dossi N, Toniolo R, Pizzariello A, Carrilho E, Piccin E, Battiston S, et al. An electrochemical gas sensor based on paper supported room temperature ionic liquids. Lab Chip 2012;12(1):153–8.

[68] Tamilarasan P, Ramaprabhu S. Graphene based all-solid-state supercapacitors with ionic liquid incorporated polyacrylonitrile electrolyte. Energy 2013;51:374–81.

[69] Ayalneh Tiruye G, Muñoz-Torrero D, Palma J, Anderson M, Marcilla R. All-solid state supercapacitors operating at 3.5 V by using ionic liquid based polymer electrolytes. J Power Sources 2015;279:472–80.

[70] Piedrahita CR, Yue P, Cao J, Lee H, Rajapaksha CP, Feng C, et al. Flexoelectricity in flexoionic polymer electrolyte membranes: effect of thiosiloxane modification on poly(ethylene glycol) diacrylate and ionic liquid electrolyte composites. ACS Appl Mater Interfaces 2020;12(14):16978–86.

[71] Cao J, Piedrahita C, Kyu T. Mechanoelectrical conversion in highly ionic conductive solid-state polymer electrolyte membranes. Macromol Mater Eng 2019;304(5):1800777.

[72] Liu Y, Lu C, Twigg S, Ghaffari M, Lin J, Winograd N, et al. Direct observation of ion distributions near electrodes in ionic polymer actuators containing ionic liquids. Sci Rep 2013;3(1):973.

[73] Feng C, Rajapaksha CPH, Cedillo JM, Piedrahita C, Cao J, Kaphle V, et al. Electroresponsive ionic liquid crystal elastomers. Macromol Rapid Commun 2019;40(19):1900299.

[74] Carmichael AJ, Hardacre C, Holbrey JD, Seddon KR, Nieuwenhuyzen M. Structure and bonding in ionic liquids. In: Trulove PC, de Long HC, Stafford GR, Deki S, editors. Molten salts XII: proceedings of the international symposium. Pennington: The Electrochemical Society; 2000. p. 209–21.

[75] Hagiwara R, Ito Y. Room temperature ionic liquids of alkylimidazolium cations and fluoroanions. J Fluor Chem 2000;105(2):221–7.

[76] Liu C, Huang N, Xu F, Tong J, Chen Z, Gui X, et al. 3D printing technologies for flexible tactile sensors toward wearable electronics and electronic skin. Polymers 2018;10(6):629.

[77] Li R, Chen G, He M, Tian J, Su B. Patternable transparent and conductive elastomers towards flexible tactile/strain sensors. J Mater Chem C 2017;5(33):8475–81.

[78] Tian K, Bae J, Bakarich SE, Yang C, Gately RD, Spinks GM, et al. 3D printing of transparent and conductive heterogeneous hydrogel–elastomer systems. Adv Mater 2017;29(10):1604827.

[79] Ha M, Lim S, Ko H. Wearable and flexible sensors for user-interactive health-monitoring devices. J Mater Chem B 2018;6(24):4043–64.

[80] Jayathilaka WADM, Qi K, Qin Y, Chinnappan A, Serrano-García W, Baskar C, et al. Significance of nanomaterials in wearables: a review on wearable actuators and sensors. Adv Mater 2019;31(7):1805921.

[81] Peng Y, Zhao L, Yang C, Yang Y, Song C, Wu Q, et al. Super tough and strong self-healing elastomers based on polyampholytes. J Mater Chem A 2018;6 (39):19066–74.

[82] Darabi MA, Khosrozadeh A, Mbeleck R, Liu Y, Chang Q, Jiang J, et al. Skin-inspired multifunctional autonomic-intrinsic conductive self-healing hydrogels with pressure sensitivity, stretchability, and 3D printability. Adv Mater 2017;29(31):1700533.

[83] Luo F, Sun TL, Nakajima T, Kurokawa T, Zhao Y, Ihsan AB, et al. Crack blunting and advancing behaviors of tough and self-healing polyampholyte hydrogel. Macromolecules 2014;47(17):6037–46.

[84] Xu K, Lu Y, Takei K. Multifunctional skin-inspired flexible sensor systems for wearable electronics. Adv Mater Technol 2019;4(3):1800628.

[85] Daemi H, Rajabi-Zeleti S, Sardon H, Barikani M, Khademhosseini A, Baharvand H. A robust super-tough biodegradable elastomer engineered by supramolecular ionic interactions. Biomaterials 2016;84:54–63.

[86] Vatani M, Vatani M, Choi JW. Multi-layer stretchable pressure sensors using ionic liquids and carbon nanotubes. Appl Phys Lett 2016;108(6):061908. Erratum in: Appl Phys Lett 2016;108(16):169902

[87] Jia H, He Y, Zhang X, Du W, Wang Y. Integrating ultra-thermal-sensitive fluids into elastomers for multifunctional flexible sensors. Adv Electron Mater 2015;1(3):1500029.

[88] Amoli V, Kim JS, Jee E, Chung YS, Kim SY, Koo J, et al. A bioinspired hydrogen bond-triggered ultrasensitive ionic mechanoreceptor skin. Nat Commun 2019;10(1):4019.

[89] Nie B, Li R, Brandt JD, Pan T. Iontronic microdroplet array for flexible ultrasensitive tactile sensing. Lab Chip 2014;14(6):1107–16.

[90] Choi D, Jang S, Kim JS, Kim HJ, Kim DH, Kwon JY. A highly sensitive tactile sensor using a pyramid-plug structure for detecting pressure, shear force, and torsion. Adv Mater Technol 2019;4(3):1800284.

[91] Sun JY, Keplinger C, Whitesides GM, Suo Z. Ionic skin. Adv Mater 2014;26 (45):7608–14.

[92] Yang JC, Mun J, Kwon SY, Park S, Bao Z, Park S. Electronic skin: recent progress and future prospects for skin-attachable devices for health monitoring, robotics, and prosthetics. Adv Mater 2019;31(48):1904765.

[93] Wang T, Farajollahi M, Choi YS, Lin IT, Marshall JE, Thompson NM, et al. Electroactive polymers for sensing. Interface. Focus 2016;6(4):20160026.

[94] Amoli V, Kim JS, Kim SY, Koo J, Chung YS, Choi H, et al. Ionic tactile sensors for emerging human-interactive technologies: a review of recent progress. Adv Funct Mater 2020;30(20):1904532.

[95] Pei Q, Inganäs O. Electrochemical applications of the bending beam method. 1. Mass transport and volume changes in polypyrrole during redox. J Phys Chem 1992;96(25):10507–14.

[96] Sugino T, Kiyohara K, Takeuchi I, Mukai K, Asaka K. Actuator properties of the complexes composed by carbon nanotube and ionic liquid: the effects of additives. Sens Actuators B 2009;141(1):179–86.

[97] Tanaka T, Nishio I, Sun ST, Ueno-Nishio S. Collapse of gels in an electric field. Science 1982;218(4571):467–9.

[98] Shahinpoor M. Ionic polymer–conductor composites as biomimetic sensors, robotic actuators and artificial muscles—a review. Electrochim Acta 2003;48 (14–16):2343–53.

[99] Choi P, Jalani NH, Datta R. Thermodynamics and proton transport in Nafion: II. Proton diffusion mechanisms and conductivity. J Electrochem Soc 2005;152(3):E123.

[100] Saccardo MC, Zuquello AG, Tozzi KA, Gonçalves R, Hirano LA, Scuracchio CH. Counter-ion and humidity effects on electromechanical properties of Nafion®/Pt composites. Mater Chem Phys 2020;244:122674.

[101] Lee JW, Yu S, Hong SM, Koo CM. High-strain air-working soft transducers produced from nanostructured block copolymer ionomer/silicate/ionic liquid nanocomposite membranes. J Mater Chem C 2013;1(24):3784–93.

[102] Yan Y, Santaniello T, Bettini LG, Minnai C, Bellacicca A, Porotti R, et al. Electroactive ionic soft actuators with monolithically integrated gold nanocomposite electrodes. Adv Mater 2017;29(23):1606109.

[103] Monobe H, Tsuchiya N, Yamamura M, Mukai K, Sugino T, Asaka K. Actuation and blocking force of carbon nanotube/polymer actuator with platelet-shaped graphene. Jpn J Appl Phys 2020;59(SD):SDDF08.

[104] Akle BJ, Bennett MD, Leo DJ. High-strain ionomeric–ionic liquid electroactive actuators. Sens Actuators A Phys 2006;126(1):173–81.

[105] Bennett MD, Leo DJ. Ionic liquids as stable solvents for ionic polymer transducers. Sens Actuators A Phys 2004;115(1):79–90.

[106] Wang J, Xu C, Taya M, Kuga Y. A Flemion-based actuator with ionic liquid as solvent. Smart Mater Struct 2007;16(2):S214–9.

[107] Kim J, Park M, Kim S, Jeon M. Effect of ionic polymer membrane with multiwalled carbon nanotubes on the mechanical performance of ionic electroactive polymer actuators. Polymers 2020;12(2):396.

[108] Yip J, Ding F, Yick KL, Yuen CWM, Lee TT, Choy WH. Tunable carbon nanotube ionic polymer actuators that are operable in dry conditions. Sens Actuators B Chem 2012;162(1):76–81.

[109] Nguyen VK, Yoo Y. A novel design and fabrication of multilayered ionic polymer–metal composite actuators based on Nafion/layered silicate and Nafion/silica nanocomposites. Sens Actuators B Chem 2007;123(1): 183–90.

[110] Lee JW, Hong SM, Kim J, Koo CM. Novel sulfonated styrenic pentablock copolymer/silicate nanocomposite membranes with controlled ion channels and their IPMC transducers. Sens Actuators B Chem 2012;162(1):369–76.

[111] Shen C, Zhao Q, Evans CM. Precise network polymerized ionic liquids for low-voltage, dopant-free soft actuators. Adv Mater Technol 2019;4(2):1800535.

[112] Kokubo H, Sano R, Murai K, Ishii S, Watanabe M. Ionic polymer actuators using poly(ionic liquid) electrolytes. Eur Polym J 2018;106:266–72.

[113] Cowan MG, Lopez AM, Masuda M, Kohno Y, McDaniel WM, Noble RD, et al. Imidazolium-based poly(ionic liquid)/ionic liquid ion-gels with high ionic conductivity prepared from a curable poly(ionic liquid). Macromol Rapid Commun 2016;37(14):1150–4.

[114] Wang F, Jeon JH, Park S, Kee CD, Kim SJ, Oh IK. A soft biomolecule actuator based on a highly functionalized bacterial cellulose nano-fiber network with carboxylic acid groups. Soft Matter 2016;12(1):246–54.

[115] Li J, Ma W, Song L, Niu Z, Cai L, Zeng Q, et al. Superfast-response and ultrahigh-power-density electromechanical actuators based on hierarchal carbon nanotube electrodes and chitosan. Nano Lett 2011;11(11):4636–41.

[116] Plesse C, Vidal F, Teyssié D, Chevrot C. Conducting polymer artificial muscle fibres: toward an open air linear actuation. Chem Commun 2010;46 (17):2910–2.

[117] Hu F, Xue Y, Xu J, Lu B. PEDOT-based conducting polymer actuators. Front Robot AI 2019;6:114.

[118] Kim KJ, Shahinpoor M. A novel method of manufacturing three-dimensional ionic polymer–metal composites (IPMCs) biomimetic sensors, actuators and artificial muscles. Polymer 2002;43(3):797–802.

[119] Shahinpoor M, Kim KJ. Ionic polymer–metal composites: I. fundamentals. Smart Mater Struct 2001;10(4):819–33.

[120] Nemat-Nasser S. Micromechanics of actuation of ionic polymer–metal composites. J Appl Phys 2002;92(5):2899–915.

[121] Wiles KB, Akle BJ, Hickner MA, Bennett M, Leo DJ, McGrath JE. Directly copolymerized poly(arylene sulfide sulfone) and poly(arylene ether sulfone) disulfonated copolymers for use in ionic polymer transducers. J Electrochem Soc 2007;154(6):P77.

[122] Nemat-Nasser S, Wu Y. Comparative experimental study of ionic polymer–metal composites with different backbone ionomers and in various cation forms. J Appl Phys 2003;93(9):5255–67.

[123] Phillips AK, Moore RB. Ionic actuators based on novel sulfonated ethylene vinyl alcohol copolymer membranes. Polymer 2005;46(18):7788–802.

[124] Duncan AJ, Leo DJ, Long TE. Beyond Nafion: charged macromolecules tailored for performance as ionic polymer transducers. Macromolecules 2008;41 (21):7765–75.

[125] Verbrugge MW, Hill RF. Analysis of promising perfluorosulfonic acid membranes for fuel-cell electrolytes. J Electrochem Soc 1990;137 (12):3770–7.

[126] Wang Y, Chen H, Wang Y, Zhu Z, Li D. Effect of dehydration on the mechanical and physicochemical properties of gold- and palladium-ionomeric polymer–metal composite (IPMC) actuators. Electrochim Acta 2014;129:450–8.

[127] Barramba J, Silva J, Costa Branco PJ. Evaluation of dielectric gel coating for encapsulation of ionic polymer–metal composite (IPMC) actuators. Sens Actuators A Phys 2007;140(2):232–8.

[128] Takeuchi I, Asaka K, Kiyohara K, Sugino T, Terasawa N, Mukai K, et al. Electromechanical behavior of fully plastic actuators based on bucky gel containing various internal ionic liquids. Electrochim Acta 2009;54 (6):1762–8.

[129] Wang XL, Oh IK, Lu J, Ju J, Lee S. Biomimetic electro-active polymer based on sulfonated poly (styrene-b-ethylene-co-butylene-b-styrene). Mater Lett 2007;61(29):5117–20.

[130] Green MD, Wang D, Hemp ST, Choi JH, Winey KI, Heflin JR, et al. Synthesis of imidazolium ABA triblock copolymers for electromechanical transducers. Polymer 2012;53(17):3677–86.

[131] Park JH, Han MJ, Song DS, Jho JY. Ionic polymer–metal composite actuators obtained from radiation-grafted cation- and anion-exchange membranes. ACS Appl Mater Interfaces 2014;6(24):22847–54.

[132] Shahinpoor M. Fundamentals of ionic polymer metal composites (IPMCs). In: Shahinpoor M, editor. Ionic polymer metal composites (IPMCs): smart multi-functional materials and artificial muscles. London: Royal Society of Chemistry; 2016. p. 1–60.

[133] Takenaka H, Torikai E, Kawami Y, Wakabayashi N. Solid polymer electrolyte water electrolysis. Int J Hydrogen Energy 1982;7(5):397–403.

[134] Nakabo Y, Mukai T, Asaka K. Biomimetic soft robots using IPMC. In: Kim KJ, Tadokoro S, editors. Electroactive polymers for robotic applications. London: Springer; 2007. p. 165–98.

[135] Tiwari R, Garcia E. The state of understanding of ionic polymer metal composite architecture: a review. Smart Mater Struct 2011;20(8):083001.

[136] Shahinpoor M, Kim KJ. Ionic polymer–metal composites: IV. industrial and medical applications. Smart Mater Struct 2004;14(1):197–214.

[137] Akle BJ, Leo DJ, Hickner MA, McGrath JE. Correlation of capacitance and actuation in ionomeric polymer transducers. J Mater Sci 2005;40 (14):3715–24.

[138] Chung CK, Fung PK, Hong YZ, Ju MS, Lin CCK, Wu TC. A novel fabrication of ionic polymer–metal composites (IPMC) actuator with silver nano-powders. Sens Actuators B Chem 2006;117(2):367–75.

[139] Tiwari R, Kim KJ. Disc-shaped ionic polymer metal composites for use in mechano-electrical applications. Smart Mater Struct 2010;19(6):065016.

[140] Jin N, Wang B, Bian K, Chen Q, Xiong K. Performance of ionic polymer–metal composite (IPMC) with different surface roughening methods. Front Mech Eng China 2009;4(4):430–5.

[141] Noh TG, Tak Y, Nam JD, Choi H. Electrochemical characterization of polymer actuator with large interfacial area. Electrochim Acta 2002;47(13–14):2341–6.

[142] Taccola S, Bellacicca A, Milani P, Beccai L, Greco F. Low-voltage dielectric elastomer actuators with stretchable electrodes fabricated by supersonic cluster beam implantation. J Appl Phys 2018;124(6):064901.

[143] Abdullayev E, Lvov Y. Halloysite clay nanotubes as a ceramic "skeleton" for functional biopolymer composites with sustained drug release. J Mater Chem B 2013;1(23):2894–903.

[144] Kim HI, Kim DK, Han JH. Study of flapping actuator modules using IPMC. In: Proceedings of the SPIE Smart Structures and Materials + Nondestructive Evaluation and Health Monitoring; 2007 Mar 18–22; San Diego, CA, USA; 2007.

[145] Lee SG, Park HC, Pandita SD, Yoo YT. Performance improvement of IPMC (ionic polymer metal composites) for a flapping actuator. Int J Control Autom Syst 2006;4(6):748–55.

[146] Suzumori K, Nabae H, Asaka K, Horiuchi T. Applying IPMC to soft robots. In: Bar-Cohen Y, Anderson IA, Shea HR, editors. Proceedings volume 11375, Electroactive Polymer Actuators and Devices (EAPAD) XXII; 2020 Apr 27–May 9; online conference. Bellingham: SPIE; 2020. p. 113750A.

[147] Chen S, Cao Y, Sarparast M, Yuan H, Dong L, Tan X, et al. Soft crawling robots: design, actuation, and locomotion. Adv Mater Technol 2020;5(2):1900837.

[148] Shen Q, Wang T, Kim KJ. A biomimetic underwater vehicle actuated by waves with ionic polymer–metal composite soft sensors. Bioinspir Biomim 2015;10 (5):055007.

[149] Chen Z. A review on robotic fish enabled by ionic polymer–metal composite artificial muscles. Robotics Biomim 2017;4(1):24.

[150] Bar-Cohen Y. Electroactive polymers: current capabilities and challenges. In: Proceedings of the SPIE's 9th Annual International Symposium on Smart Structures and Materials; 2002 Mar 17–21; San Diego, CA, USA; 2002.

[151] Okuzaki H, Kuwabara T, Funasaka K, Saido T. Humidity-sensitive polypyrrole films for electro-active polymer actuators. Adv Funct Mater 2013;23 (36):4400–7.

[152] Sansiñena JM, Gao J, Wang HL. High-performance, monolithic polyaniline electrochemical actuators. Adv Funct Mater 2003;13(9):703–9.

[153] Kim J, Yun SR, Deshpande SD. Synthesis, characterization and actuation behavior of polyaniline-coated electroactive paper actuators. Polym Int 2007;56(12):1530–6.

[154] Kotal M, Kim J, Kim KJ, Oh IK. Sulfur and nitrogen Co-doped graphene electrodes for high-performance ionic artificial muscles. Adv Mater 2016;28 (8):1610–5.

[155] Wang D, Lu C, Zhao J, Han S, Wu M, Chen W. High energy conversion efficiency conducting polymer actuators based on PEDOT:PSS/MWCNTs composite electrode. RSC Adv 2017;7(50):31264–71.

[156] Skotheim TA, Reynolds JR. Handbook of conducting polymers. 3rd ed. Boca Raton: CRC Press; 2007.

[157] Moliton A, Hiorns RC. Review of electronic and optical properties of semiconducting π-conjugated polymers: applications in optoelectronics. Polym Int 2004;53(10):1397–412.

[158] Lund A, Darabi S, Hultmark S, Ryan JD, Andersson B, Ström A, et al. Roll-to-roll dyed conducting silk yarns: a versatile material for e-textile devices. Adv Mater Technol 2018;3(12):1800251.

[159] Põldsalu I, Rohtlaid K, Nguyen TMG, Plesse C, Vidal F, Khorram MS, et al. Thin ink-jet printed trilayer actuators composed of PEDOT:PSS on interpenetrating polymer networks. Sens Actuators B Chem 2018;258:1072–9.

[160] Zolfagharian A, Kouzani AZ, Khoo SY, Moghadam AAA, Gibson I, Kaynak A. Evolution of 3D printed soft actuators. Sens Actuators A Phys 2016;250:258–72.

[161] Shalu S, Singh VK, Singh RK. Development of ion conducting polymer gel electrolyte membranes based on polymer PVdF-HFP, BMIMTFSI ionic liquid and the Li-salt with improved electrical, thermal and structural properties. J Mater Chem C 2015;3(28):7305–18.

[162] Zhou D, Spinks GM, Wallace GG, Tiyapiboonchaiya C, MacFarlane DR, Forsyth M, et al. Solid state actuators based on polypyrrole and polymer-in-ionic liquid electrolytes. Electrochim Acta 2003;48(14–16):2355–9.

[163] Park M, Kim J, Song H, Kim S, Jeon M. Fast and stable ionic electroactive polymer actuators with PEDOT:PSS/graphene–Ag-nanowires) nanocomposite electrodes. Sensors 2018;18(9):3126.

[164] Melling D, Martinez JG, Jager EWH. Conjugated polymer actuators and devices: progress and opportunities. Adv Mater 2019;31(22):1808210.

[165] Cheedarala RK, Jeon JH, Kee CD, Oh IK. Bio-inspired all-organic soft actuator based on a π–π stacked 3D ionic network membrane and ultra-fast solution processing. Adv Funct Mater 2014;24(38):6005–15.

[166] Vidal F, Plesse C, Teyssié D, Chevrot C. Long-life air working conducting semi-IPN/ionic liquid based actuator. Synth Met 2004;142(1–3):287–91.

[167] Festin N, Maziz A, Plesse C, Teyssié D, Chevrot C, Vidal F. Robust solid polymer electrolyte for conducting IPN actuators. Smart Mater Struct 2013;22 (10):104005.

[168] Woehling V, Nguyen GTM, Plesse C, Cantin S, Madden JDW, Vidal F. Interpenetrating polymer network (IPN) as tool for tuning electromechanical properties of electrochemical actuator operating in open-air. Sens Actuators B Chem 2018;256:294–303.

[169] Woehling V, Nguyen GTM, Plesse C, Farajollahi M, Madden JDW, Vidal F. Toward electroactive catheter design using conducting interpenetrating polymer networks actuators. In: Bar-Cohen Y, editor. Proceedings volume 10594, Electroactive Polymer Actuators and Devices (EAPAD) XX; 2018 Mar 4–8; Denver, CO, USA. Bellingham: SPIE; 2018. p. 1059415.

[170] Farajollahi M, Woehling V, Plesse C, Nguyen GTM, Vidal F, Sassani F, et al. Self-contained tubular bending actuator driven by conducting polymers. Sens Actuators A Phys 2016;249:45–56.

[171] Maziz A, Concas A, Khaldi A, Stålhand J, Persson NK, Jager EWH. Knitting and weaving artificial muscles. Sci Adv 2017;3(1):e1600327.

[172] Maziz A, Plesse C, Soyer C, Chevrot C, Teyssié D, Cattan E, et al. Demonstrating kHz frequency actuation for conducting polymer microactuators. Adv Funct Mater 2014;24(30):4851–9.

[173] Kim SS, Jeon JH, Kee CD, Oh IK. Electro-active hybrid actuators based on freeze-dried bacterial cellulose and PEDOT:PSS. Smart Mater Struct 2013;22 (8):085026.

[174] Khan A, Abas Z, Kim HS, Kim J. Recent progress on cellulose-based electro-active paper, its hybrid nanocomposites and applications. Sensors 2016;16 (8):1172.

[175] Mirvakili SM, Hunter IW. Artificial muscles: mechanisms, applications, and challenges. Adv Mater 2018;30(6):1704407.

[176] Taccola S, Greco F, Sinibaldi E, Mondini A, Mazzolai B, Mattoli V. Toward a new generation of electrically controllable hygromorphic soft actuators. Adv Mater 2015;27(10):1668–75.

[177] Liu S, Liu Y, Cebeci H, de Villoria RG, Lin JH, Wardle BL, et al. High electromechanical response of ionic polymer actuators with controlled-morphology aligned carbon nanotube/Nafion nanocomposite electrodes. Adv Funct Mater 2010;20(19):3266–71.

[178] Kim J, Jeon JH, Kim HJ, Lim H, Oh IK. Durable and water-floatable ionic polymer actuator with hydrophobic and asymmetrically laser-scribed reduced graphene oxide paper electrodes. ACS Nano 2014;8(3):2986–97.

[179] Xie X, Qu L, Zhou C, Li Y, Zhu J, Bai H, et al. An asymmetrically surface-modified graphene film electrochemical actuator. ACS Nano 2010;4 (10):6050–4.

[180] Wang H, Liu B, Wang L, Chen X, Chen Z, Qi Y, et al. Graphene glass inducing multidomain orientations in cholesteric liquid crystal devices toward wide viewing angles. ACS Nano 2018;12(7):6443–51.

[181] Lu C, Yang Y, Chen X. Ultra-thin conductive graphitic carbon nitride assembly through van der Waals epitaxy toward high-energy-density flexible supercapacitors. Nano Lett 2019;19(6):4103–11.

[182] Lu C, Chen X. Flexible and electroactive ionogel graphene composite actuator. Materials 2020;13(3):656.

[183] Asaka K, Mukai K, Sugino T, Kiyohara K. Ionic electroactive polymer actuators based on nano-carbon electrodes. Polym Int 2013;62(9):1263–70.

[184] Baughman RH, Cui C, Zakhidov AA, Iqbal Z, Barisci JN, Spinks GM, et al. Carbon nanotube actuators. Science 1999;284(5418):1340–4.

[185] Fukushima T, Kosaka A, Ishimura Y, Yamamoto T, Takigawa T, Ishii N, et al. Molecular ordering of organic molten salts triggered by single-walled carbon nanotubes. Science 2003;300(5628):2072–4.

[186] Mukai K, Asaka K, Kiyohara K, Sugino T, Takeuchi I, Fukushima T, et al. High performance fully plastic actuator based on ionic-liquid-based bucky gel. Electrochim Acta 2008;53(17):5555–62.

[187] Mukai K, Asaka K, Sugino T, Kiyohara K, Takeuchi I, Terasawa N, et al. Highly conductive sheets from millimeter-long single-walled carbon nanotubes and ionic liquids: application to fast-moving, low-voltage electromechanical actuators operable in air. Adv Mater 2009;21(16):1582–5.

[188] Hata K, Futaba DN, Mizuno K, Namai T, Yumura M, Iijima S. Water-assisted highly efficient synthesis of impurity-free single-walled carbon nanotubes. Science 2004;306(5700):1362–4.

[189] Torop J, Sugino T, Asaka K, Jänes A, Lust E, Aabloo A. Nanoporous carbide-derived carbon based actuators modified with gold foil: prospect for fast response and low voltage applications. Sens Actuators B Chem 2012;161 (1):629–34.

[190] Must I, Kaasik F, Põldsalu I, Johanson U, Punning A, Aabloo A. A carbide-derived carbon laminate used as a mechanoelectrical sensor. Carbon 2012;50 (2):535–41.

[191] Kaasik F, Must I, Baranova I, Põldsalu I, Lust E, Johanson U, et al. Scalable fabrication of ionic and capacitive laminate actuators for soft robotics. Sens Actuators B Chem 2017;246:154–63.

[192] Takeuchi I, Asaka K, Kiyohara K, Sugino T, Terasawa N, Mukai K, et al. Electromechanical behavior of a fully plastic actuator based on dispersed nano-carbon/ionic-liquid-gel electrodes. Carbon 2009;47(5):1373–80.

[193] Palmre V, Lust E, Jänes A, Koel M, Peikolainen AL, Torop J, et al. Electroactive polymer actuators with carbon aerogel electrodes. J Mater Chem 2011;21 (8):2577–83.

[194] Cottinet PJ, Souders C, Tsai SY, Liang R, Wang B, Zhang C. Electromechanical actuation of buckypaper actuator: material properties and performance relationships. Phys Lett A 2012;376(12–13):1132–6.

[195] Palmre V, Brandell D, Mäeorg U, Torop J, Volobujeva O, Punning A, et al. Nanoporous carbon-based electrodes for high strain ionomeric bending actuators. Smart Mater Struct 2009;18(9):095028.

[196] Sugino T, Kiyohara K, Takeuchi I, Mukai K, Asaka K. Improving the actuating response of carbon nanotube/ionic liquid composites by the addition of conductive nanoparticles. Carbon 2011;49(11):3560–70.

[197] Mukai K, Asaka K, Hata K, Otero TF, Oike H. High-speed carbon nanotube actuators based on an oxidation/reduction reaction. Chemistry 2011;17 (39):10965–71.

[198] Kim J, Bae SH, Kotal M, Stalbaum T, Kim KJ, Oh IK. Soft but powerful artificial muscles based on 3D graphene–CNT–Ni heteronanostructures. Small 2017;13(31):1701314.

[199] Wu G, Wu X, Xu Y, Cheng H, Meng J, Yu Q, et al. High-performance hierarchical black-phosphorous-based soft electrochemical actuators in bioinspired applications. Adv Mater 2019;31(25):1806492.

[200] Lu L, Liu J, Hu Y, Zhang Y, Chen W. Graphene-stabilized silver nanoparticle electrochemical electrode for actuator design. Adv Mater 2013;25(9):1270–4.

[201] Umrao S, Tabassian R, Kim J, Nguyen VH, Zhou Q, Nam S, et al. MXene artificial muscles based on ionically cross-linked Ti$_3$C$_2$T$_x$ electrode for kinetic soft robotics. Sci Robot 2019;4(33):eaaw7797.

[202] Lian Y, Liu Y, Jiang T, Shu J, Lian H, Cao M. Enhanced electromechanical performance of graphite oxide–Nafion nanocomposite actuator. J Phys Chem C 2010;114(21):9659–63.

[203] Ying Z, Wang Q, Xie J, Li B, Lin X, Hui S. Novel electrically-conductive electro-responsive hydrogels for smart actuators with a carbon-nanotube-enriched three-dimensional conductive network and a physical-phase-type three-dimensional interpenetrating network. J Mater Chem C 2020;8 (12):4192–205.

[204] Asaka K, Oguro K. Active microcatheter and biomedical soft devices based on IPMC actuators. In: Carpi F, Smela E, editors. Biomedical applications of electroactive polymer actuators. Chichester: John Wiley & Sons, Ltd.; 2009. p. 121–36.

[205] Annabestani M, Fardmanesh M. Ionic electro active polymer-based soft actuators and their applications in microfluidic micropumps, microvalves, and micromixers: a review. 2019. arXiv:1904.07149.

[206] Bhandari B, Lee GY, Ahn SH. A review on IPMC material as actuators and sensors: fabrications, characteristics and applications. Int J Precis Eng Manuf 2012;13(1):141–63.

[207] Zhang Z, Demir KG, Gu GX. Developments in 4D-printing: a review on current smart materials, technologies, and applications. Int J Smart Nano Mater 2019;10(3):205–24.

[208] Boldini A, Porfiri M. Multiaxial deformations of ionic polymer metal composites. Int J Eng Sci 2020;149:103227.

[209] Zolfagharian A, Kaynak A, Bodaghi M, Kouzani AZ, Gharaie S, Nahavandi S. Control-based 4D printing: adaptive 4D-printed systems. Appl Sci 2020;10 (9):3020.

[210] Kruusamäe K, Punning A, Aabloo A, Asaka K. Self-sensing ionic polymer actuators: a review. Actuators 2015;4(1):17–38.

[211] Mohdlsa WH, Hunt A, HosseinNia SH. Sensing and self-sensing actuation methods for ionic polymer–metal composite (IPMC): a review. Sensors 2019;19(18):3967.

[212] Vermes B, Czigany T. Non-conventional deformations: materials and actuation. Materials 2020;13(6):1383.

[213] Bashir M, Rajendran P. A review on electroactive polymers development for aerospace applications. J Intell Mater Syst Struct 2018;29(19):3681–95.

[214] Walsh C. Human-in-the-loop development of soft wearable robots. Nat Rev Mater 2018;3(6):78–80.

[215] Sherif HMF. The artificial ventricle: a conceptual design for a novel mechanical circulatory support system. Minim Invasive Ther Allied Technol 2009;18(3):178–80.

[216] Sawa Y, Urayama K, Takigawa T, DeSimone A, Teresi L. Thermally driven giant bending of liquid crystal elastomer films with hybrid alignment. Macromolecules 2010;43(9):4362–9.

[217] Mol GN, Harris KD, Bastiaansen CWM, Broer DJ. Thermo-mechanical responses of liquid-crystal networks with a splayed molecular organization. Adv Funct Mater 2005;15(7):1155–9.

[218] Ryu S, Lee P, Chou JB, Xu R, Zhao R, Hart AJ, et al. Extremely elastic wearable carbon nanotube fiber strain sensor for monitoring of human motion. ACS Nano 2015;9(6):5929–36.

[219] Roh E, Hwang BU, Kim D, Kim BY, Lee NE. Stretchable, transparent, ultrasensitive, and patchable strain sensor for human–machine interfaces comprising a nanohybrid of carbon nanotubes and conductive elastomers. ACS Nano 2015;9(6):6252–61.

[220] Yamada T, Hayamizu Y, Yamamoto Y, Yomogida Y, Izadi-Najafabadi A, Futaba DN, et al. A stretchable carbon nanotube strain sensor for human-motion detection. Nat Nanotechnol 2011;6(5):296–301.

[221] Majidi C, Kramer R, Wood RJ. A non-differential elastomer curvature sensor for softer-than-skin electronics. Smart Mater Struct 2011;20(10):105017.

[222] Dickey MD, Chiechi RC, Larsen RJ, Weiss EA, Weitz DA, Whitesides GM. Eutectic gallium–indium (EGaIn): a liquid metal alloy for the formation of stable structures in microchannels at room temperature. Adv Funct Mater 2008;18(7):1097–104.

[223] Gong S, Lai DTH, Su B, Si KJ, Ma Z, Yap LW, et al. Highly stretchy black gold e-skin nanopatches as highly sensitive wearable biomedical sensors. Adv Electron Mater 2015;1(4):1400063.

[224] Wu JM, Chen CY, Zhang Y, Chen KH, Yang Y, Hu Y, et al. Ultrahigh sensitive piezotronic strain sensors based on a ZnSnO$_3$ nanowire/microwire. ACS Nano 2012;6(5):4369–74.

[225] Xiao X, Yuan L, Zhong J, Ding T, Liu Y, Cai Z, et al. High-strain sensors based on ZnO nanowire/polystyrene hybridized flexible films. Adv Mater 2011;23 (45):5440–4.

[226] Yao S, Zhu Y. Wearable multifunctional sensors using printed stretchable conductors made of silver nanowires. Nanoscale 2014;6(4):2345–52.

[227] Amjadi M, Pichitpajongkit A, Lee S, Ryu S, Park I. Highly stretchable and sensitive strain sensor based on silver nanowire–elastomer nanocomposite. ACS Nano 2014;8(5):5154–63.

[228] Lee J, Kim S, Lee J, Yang D, Park BC, Ryu S, et al. A stretchable strain sensor based on a metal nanoparticle thin film for human motion detection. Nanoscale 2014;6(20):11932–9.

[229] Segev-Bar M, Haick H. Flexible sensors based on nanoparticles. ACS Nano 2013;7(10):8366–78.

[230] Megha R, Ali FA, Ravikiran YT, Ramana CHVV, Kiran Kumar ABV, Mishra DK, et al. Conducting polymer nanocomposite based temperature sensors: a review. Inorg Chem Commun 2018;98:11–28.

[231] Faridbod F, Norouzi P, Dinarvand R, Ganjali MR. Developments in the field of conducting and non-conducting polymer based potentiometric membrane sensors for ions over the past decade. Sensors 2008;8(4):2331–412.

[232] Saylan Y, Akgönüllü S, Yavuz H, Ünal S, Denizli A. Molecularly imprinted polymer based sensors for medical applications. Sensors 2019;19(6):1279.

[233] Gerboni G, Diodato A, Ciuti G, Cianchetti M, Menciassi A. Feedback control of soft robot actuators via commercial flex bend sensors. IEEE/ASME Trans Mechatron 2017;22(4):1881–8.

[234] Saggio G. A novel array of flex sensors for a goniometric glove. Sens Actuators A Phys 2014;205:119–25.

[235] Chortos A, Bao Z. Skin-inspired electronic devices. Mater Today 2014;17 (7):321–31.

[236] Zhao J, Dai K, Liu C, Zheng G, Wang B, Liu C, et al. A comparison between strain sensing behaviors of carbon black/polypropylene and carbon nanotubes/polypropylene electrically conductive composites. Compos Part A-Appl S 2013;48:129–36.

[237] Wichmann MHG, Buschhorn ST, Böger L, Adelung R, Schulte K. Direction sensitive bending sensors based on multi-wall carbon nanotube/epoxy nanocomposites. Nanotechnology 2008;19(47):475503.

[238] Neely JS, Restle PJ, inventors; International Business Machines Corporation, assignee. Capacitive bend sensor. United States patent US 5610528. 1997 Mar 11.

[239] Manandhar P, Calvert PD, Buck JR. Elastomeric ionic hydrogel sensor for large strains. IEEE Sens J 2012;12(6):2052–61.

[240] Klapper R, Upham P. The impact of micro-firm everyday practices on sustainable development in local communities. In: Kyrö P, editor. Handbook of entrepreneurship and sustainable development research. Cheltenham: Edward Elgar Publishing; 2015. p. 275–95.

[241] Metzger C, Fleisch E, Meyer J, Dansachmüller M, Graz I, Kaltenbrunner M, et al. Flexible-foam-based capacitive sensor arrays for object detection at low cost. Appl Phys Lett 2008;92(1):013506.

[242] Gisby TA, O'Brien BM, Anderson IA. Self sensing feedback for dielectric elastomer actuators. Appl Phys Lett 2013;102(19):193703.

[243] Kollosche M, Stoyanov H, Laflamme S, Kofod G. Strongly enhanced sensitivity in elastic capacitive strain sensors. J Mater Chem 2011;21(23):8292–4.

[244] Ding Y, Xu T, Onyilagha O, Fong H, Zhu Z. Recent advances in flexible and wearable pressure sensors based on piezoresistive 3D monolithic conductive sponges. ACS Appl Mater Interfaces 2019;11(7):6685–704.

[245] Wang X, Dong L, Zhang H, Yu R, Pan C, Wang ZL. Recent progress in electronic skin. Adv Sci 2015;2(10):1500169.

[246] Hammock ML, Chortos A, Tee BCK, Tok JBH, Bao Z. 25th anniversary article: the evolution of electronic skin (e-skin): a brief history, design considerations, and recent progress. Adv Mater 2013;25(42):5997–6038.

[247] Qiu L, Bulut Coskun M, Tang Y, Liu JZ, Alan T, Ding J, et al. Ultrafast dynamic piezoresistive response of graphene-based cellular elastomers. Adv Mater 2016;28(1):194–200.

[248] Lv L, Zhang P, Xu T, Qu L. Ultrasensitive pressure sensor based on an ultralight sparkling graphene block. ACS Appl Mater Interfaces 2017;9(27):22885–92.

[249] Biddiss E, Chau T. Electroactive polymeric sensors in hand prostheses: bending response of an ionic polymer metal composite. Med Eng Phys 2006;28(6):568–78.

[250] John SW, Alici G, Spinks GM, Madden JD, Wallace GG. Towards fully optimized conducting polymer bending sensors: the effect of geometry. Smart Mater Struct 2009;18(8):085007.

[251] Lee CK, Moon FC. Laminated piezopolymer plates for torsion and bending sensors and actuators. J Acoust Soc Am 1989;85(6):2432–9.

[252] Albehaijan HA, Piedrahita CR, Cao J, Soliman M, Mitra S, Kyu T. Mechanoelectrical transduction of polymer electrolyte membranes: effect of branched networks. ACS Appl Mater Interfaces 2020;12(6):7518–28.

[253] Di Pasquale G, Graziani S, Pollicino A, Strazzeri S. A vortex-shedding flowmeter based on IPMCs. Smart Mater Struct 2016;25(1):015011.

[254] Kocer B, Zangrilli U, Akle B, Weiland L. Experimental and theoretical investigation of ionic polymer transducers in shear sensing. J Intell Mater Syst Struct 2015;26(15):2042–54.

[255] Xie R, Xie Y, López-Barrón CR, Gao KZ, Wagner NJ. Ultra-stretchable conductive iono-elastomer and motion strain sensor system developed therefrom. Technol Innov 2018;19(3):613–26.

[256] Xie Y, Xie R, Yang HC, Chen Z, Hou J, López-Barrón CR, et al. Iono-elastomer-based wearable strain sensor with real-time thermomechanical dual response. ACS Appl Mater Interfaces 2018;10(38):32435–43.

[257] Yao S, Zhu Y. Nanomaterial-enabled stretchable conductors: strategies, materials and devices. Adv Mater 2015;27(9):1480–511.

[258] Xu F, Zhu Y. Highly conductive and stretchable silver nanowire conductors. Adv Mater 2012;24(37):5117–22.

[259] Ahmed EM. Hydrogel: preparation, characterization, and applications: a review. J Adv Res 2015;6(2):105–21.

[260] Bai Y, Chen B, Xiang F, Zhou J, Wang H, Suo Z. Transparent hydrogel with enhanced water retention capacity by introducing highly hydratable salt. Appl Phys Lett 2014;105(15):151903.

[261] Larson C, Peele B, Li S, Robinson S, Totaro M, Beccai L, et al. Highly stretchable electroluminescent skin for optical signaling and tactile sensing. Science 2016;351(6277):1071–4.

[262] Le Bideau J, Viau L, Vioux A. Ionogels, ionic liquid based hybrid materials. Chem Soc Rev 2011;40(2):907–25.

[263] Marr PC, Marr AC. Ionic liquid gel materials: applications in green and sustainable chemistry. Green Chem 2016;18(1):105–28.

[264] Ding Y, Zhang J, Chang L, Zhang X, Liu H, Jiang L. Preparation of high-performance ionogels with excellent transparency, good mechanical strength, and high conductivity. Adv Mater 2017;29(47):1704253.

[265] Li M, Li J, Na H, Vlassak JJ. Mechanical behavior of poly(methyl methacrylate)-based ionogels. Soft Matter 2014;10(40):7993–8000.

[266] Chen B, Lu JJ, Yang CH, Yang JH, Zhou J, Chen YM, et al. Highly stretchable and transparent ionogels as nonvolatile conductors for dielectric elastomer transducers. ACS Appl Mater Interfaces 2014;6(10):7840–5.

[267] Robinson SS, O'Brien KW, Zhao H, Peele BN, Larson CM, Mac Murray BC, et al. Integrated soft sensors and elastomeric actuators for tactile machines with kinesthetic sense. Extreme Mech Lett 2015;5:47–53.

[268] Crump MR, Gong AT, Chai D, Bidinger SL, Pavinatto FJ, Reihsen TE, et al. Monolithic 3D printing of embeddable and highly stretchable strain sensors using conductive ionogels. Nanotechnology 2019;30(36):364002.

[269] Narongthong J, Le HH, Das A, Sirisinha C, Wießner S. Ionic liquid enabled electrical-strain tuning capability of carbon black based conductive polymer composites for small-strain sensors and stretchable conductors. Compos Sci Technol 2019;174:202–11.

[270] Homayounfar SZ, Andrew TL. Wearable sensors for monitoring human motion: a review on mechanisms, materials, and challenges. SLAS Technol 2020;25(1):9–24.

[271] Wang X, Gu Y, Xiong Z, Cui Z, Zhang T. Silk-molded flexible, ultrasensitive, and highly stable electronic skin for monitoring human physiological signals. Adv Mater 2014;26(9):1336–42.

[272] Zhu B, Niu Z, Wang H, Leow WR, Wang H, Li Y, et al. Microstructured graphene arrays for highly sensitive flexible tactile sensors. Small 2014;10(18):3625–31.

[273] Jung S, Kim JH, Kim J, Choi S, Lee J, Park I, et al. Reverse-micelle-induced porous pressure-sensitive rubber for wearable human–machine interfaces. Adv Mater 2014;26(28):4825–30.

[274] Yao HB, Ge J, Wang CF, Wang X, Hu W, Zheng ZJ, et al. A flexible and highly pressure-sensitive graphene–polyurethane sponge based on fractured microstructure design. Adv Mater 2013;25(46):6692–8.

[275] Lee S, Reuveny A, Reeder J, Lee S, Jin H, Liu Q, et al. A transparent bending-insensitive pressure sensor. Nat Nanotechnol 2016;11(5):472–8.

[276] Wang Q, Jian M, Wang C, Zhang Y. Carbonized silk nanofiber membrane for transparent and sensitive electronic skin. Adv Funct Mater 2017;27(9):1605657.

[277] Shi L, Zhu T, Gao G, Zhang X, Wei W, Liu W, et al. Highly stretchable and transparent ionic conducting elastomers. Nat Commun 2018;9(1):2630.

[278] Lee J, Faruk Emon MO, Vatani M, Choi JW. Effect of degree of crosslinking and polymerization of 3D printable polymer/ionic liquid composites on performance of stretchable piezoresistive sensors. Smart Mater Struct 2017;26(3):035043.

[279] Emon MOF, Lee J, Choi UH, Kim DH, Lee KC, Choi JW. Characterization of a soft pressure sensor on the basis of ionic liquid concentration and thickness of the piezoresistive layer. IEEE Sens J 2019;19(15):6076–84.

[280] Emon MOF, Alkadi F, Philip DG, Kim DH, Lee KC, Choi JW. Multi-material 3D printing of a soft pressure sensor. Addit Manuf 2019;28:629–38.

[281] Peng S, Li Y, Wu L, Zhong J, Weng Z, Zheng L, et al. 3D printing mechanically robust and transparent polyurethane elastomers for stretchable electronic sensors. ACS Appl Mater Interfaces 2020;12(5):6479–88.

[282] Charaya H, La TG, Rieger J, Chung HJ. Thermochromic and piezocapacitive flexible sensor array by combining composite elastomer dielectrics and transparent ionic hydrogel electrodes. Adv Mater Technol 2019;4(9):1900327.

[283] Qiu Z, Wan Y, Zhou W, Yang J, Yang J, Huang J, et al. Ionic skin with biomimetic dielectric layer templated from *Calathea Zebrine* leaf. Adv Funct Mater 2018;28(37):1802343.

[284] Chhetry A, Kim J, Yoon H, Park JY. Ultrasensitive interfacial capacitive pressure sensor based on a randomly distributed microstructured iontronic film for wearable applications. ACS Appl Mater Interfaces 2019;11(3):3438–49.

[285] Cho SH, Lee SW, Yu S, Kim H, Chang S, Kang D, et al. Micropatterned pyramidal ionic gels for sensing broad-range pressures with high sensitivity. ACS Appl Mater Interfaces 2017;9(11):10128–35.

[286] Jin ML, Park S, Lee Y, Lee JH, Chung J, Kim JS, et al. An ultrasensitive, visco-poroelastic artificial mechanotransducer skin inspired by Piezo2 protein in mammalian Merkel cells. Adv Mater 2017;29(13):1605973.

[287] Chun KY, Son YJ, Han CS. Highly sensitive and patchable pressure sensors mimicking ion-channel-engaged sensory organs. ACS Nano 2016;10(4):4550–8.

[288] Schrenk-Siemens K, Wende H, Prato V, Song K, Rostock C, Loewer A, et al. Piezo2 is required for mechanotransduction in human stem cell-derived touch receptors. Nat Neurosci 2015;18(1):10–6.

[289] Woo SH, Ranade S, Weyer AD, Dubin AE, Baba Y, Qiu Z, et al. Piezo2 is required for Merkel-cell mechanotransduction. Nature 2014;509(7502):622–6.

[290] Cho KJ, Koh JS, Kim S, Chu WS, Hong Y, Ahn SH. Review of manufacturing processes for soft biomimetic robots. Int J Precis Eng Manuf 2009;10(3):171–81.

[291] Miriyev A, Stack K, Lipson H. Soft material for soft actuators. Nat Commun 2017;8(1):596.

[292] Palagi S, Fischer P. Bioinspired microrobots. Nat Rev Mater 2018;3(6):113–24.

[293] Cianchetti M, Laschi C, Menciassi A, Dario P. Biomedical applications of soft robotics. Nat Rev Mater 2018;3(6):143–53.

[294] Sitti M. Miniature soft robots—road to the clinic. Nat Rev Mater 2018;3(6):74–5.

[295] Trivedi D, Rahn CD, Kier WM, Walker ID. Soft robotics: biological inspiration, state of the art, and future research. Appl Bionics Biomech 2008;5(3):99–117.

[296] Rus D, Tolley MT. Design, fabrication and control of soft robots. Nature 2015;521(7553):467–75.

[297] Tolley MT, Shepherd RF, Mosadegh B, Galloway KC, Wehner M, Karpelson M, et al. A resilient, untethered soft robot. Soft Robot 2014;1(3):213–23.

[298] Mazzolai B, Margheri L, Cianchetti M, Dario P, Laschi C. Soft-robotic arm inspired by the octopus: II. from artificial requirements to innovative technological solutions. Bioinspir Biomim 2012;7(2):025005.

[299] Margheri L, Laschi C, Mazzolai B. Soft robotic arm inspired by the octopus: I. from biological functions to artificial requirements. Bioinspir Biomim 2012;7(2):025004.

[300] Majidi C. Soft robotics: a perspective—current trends and prospects for the future. Soft Robot 2014;1(1):5–11.

[301] Xie M, Hisano K, Zhu M, Toyoshi T, Pan M, Okada S, et al. Flexible multifunctional sensors for wearable and robotic applications. Adv Mater Technol 2019;4(3):1800626.

[302] Chen J, Zheng J, Gao Q, Zhang J, Zhang J, Omisore OM, et al. Polydimethylsiloxane (PDMS)-based flexible resistive strain sensors for wearable applications. Appl Sci 2018;8(3):345.

[303] Wang Y, Gong S, Wang SJ, Simon GP, Cheng W. Volume-invariant ionic liquid microbands as highly durable wearable biomedical sensors. Mater Horiz 2016;3(3):208–13.

[304] Nam SH, Jeon PJ, Min SW, Lee YT, Park EY, Im S. Highly sensitive non-classical strain gauge using organic heptazole thin-film transistor circuit on a flexible substrate. Adv Funct Mater 2014;24(28):4413–9.

[305] Jeong JW, Yeo WH, Akhtar A, Norton JJS, Kwack YJ, Li S, et al. Materials and optimized designs for human–machine interfaces via epidermal electronics. Adv Mater 2013;25(47):6839–46.

[306] Park JJ, Hyun WJ, Mun SC, Park YT, Park OO. Highly stretchable and wearable graphene strain sensors with controllable sensitivity for human motion monitoring. ACS Appl Mater Interfaces 2015;7(11):6317–24.